

Dispersion of electromagnetic waves in stratified and nonstationary media (exactly solvable models)

A B Shvartsburg

DOI: 10.1070/PU2000v043n12ABEH000827

Contents

1. Introduction. Optics of nonsinusoidal waves	1201
2. Nonlocal dispersion of stratified media. Phase coordinate method	1203
3. When does the WKB approximation yield exact solutions of the wave equation?	1207
4. Broadband reflectionless properties of nonuniform dielectric layers	1207
5. Effects of the gradient and the curvature of the $\varepsilon(z)$ profile on the nonlocal dispersion of periodic nonsinusoidal dielectric structures	1210
6. Dispersion of high-frequency waves in plasmas with monotonic and nonmonotonic density distributions	1212
7. Surface electromagnetic waves in a nonuniform dielectric	1216
8. Dispersion properties of nonstationary dielectrics	1218
9. Telegraph equation for media with time-dependent conductivities	1222
10. Conclusions. Phase coordinates in problems of the radiophysics of guidance systems, nonlinear optics, and quantum mechanics	1224
References	1227

Abstract. The propagation and reflection of electromagnetic waves in stratified and nonstationary media are considered on the basis of a unified approach, using exact analytical solutions of Maxwell's equations. In this approach, the spatial structure of a wave field in an inhomogeneous medium is presented as a function of the optical path length of the wave (a one-dimensional problem). These solutions predict strong dispersion of both normal and abnormal types to occur in a given medium, the magnitude of dispersion depending on the gradient and curvature of the continuous smooth profile of the material's inhomogeneous dielectric susceptibility $\varepsilon(z)$. The effect of such a nonlocal dispersion on the reflection of waves is described by generalized Fresnel formulas. Exactly solvable models are introduced to describe the effects of both monotonic and oscillatory $\varepsilon(t)$ dependences on the wave dispersion due to the finite relaxation time of the dielectric constant.

1. Introduction. Optics of nonsinusoidal waves

This review is devoted to the effects of optical and radio wave dispersion in a dielectric medium, which arise due to the spatial nonuniformity or the temporal relaxation of its dielectric properties. The variable velocity of propagation of the wave fields in such a medium can completely change the

spectra of wave reflection and the spatiotemporal field structure within the medium. The dependences of permittivity on the coordinates and time, which are described by continuous and smooth functions of these variables, determine the domain of existence of nonlocal dispersion. For certain values of the characteristic spatial nonuniformity scales and relaxation times, this domain can be formed in a frequency range remote from the natural resonances and absorption bands of the material. Investigations into these effects in different parts of the spectrum of electromagnetic waves gain impetus from the problems of geophysics, semiconductor and polymer optics, and the physics of laboratory and cosmic plasmas. Harnessing materials with a strong artificial dispersion opens up new avenues for the synthesis of optoelectronic and radio engineering systems, the development of nondestructive testing of complex materials, and the elaboration of optimal modes of communication and energy transfer through stratified and nonstationary media. Moreover, the physical foundations and the mathematical apparatus of the theory of electromagnetic waves in such media are of interest in the analysis of wave fields in other branches of the physics of continuous media.

The effect of nonlocal dispersion on the propagation and reflection of electromagnetic waves in stratified and nonstationary media can be conveniently considered with the aid of model dependences of the medium permittivity ε on the coordinates, $\varepsilon(\mathbf{r})$, and time, $\varepsilon(t)$. While discussing one-dimensional problems for stratified media, there is good reason to note several models of $\varepsilon(z)$ which allow exact analytical solutions of the Maxwell equations. The same $\varepsilon(z)$ dependences constitute exactly solvable models for the wave equation in a medium with a variable wave velocity $v^2(z) \sim [\varepsilon(z)]^{-1}$. One of the first such profiles $v(z)$ was found by Rayleigh in 1880 in the solution of the acoustic problem of the

A B Shvartsburg Scientific and Technological Center for Unique Instrumentation, Russian Academy of Sciences, ul. Butlerova 15, 117342 Moscow, Russian Federation E-mail: alexshvarts@mtu-net.ru

Received 21 July 2000, revised 27 September 2000
Uspekhi Fizicheskikh Nauk 170 (12) 1297–1324 (2000)
 Translated by E N Ragozin; edited by A V Getling

structure of a sound field propagating with a coordinate-dependent velocity [1]:

$$\frac{v^2(z)}{v^2(z=0)} = \left(1 + \frac{z}{L}\right)^2 = \frac{\varepsilon(z=0)}{\varepsilon(z)}. \quad (1.1)$$

Here, the characteristic length L is the only free model parameter. There also exists an exact solution for a more gently sloping $\varepsilon(z)$ profile [2]:

$$\frac{\varepsilon(z)}{\varepsilon(z=0)} = \left(1 + \frac{z}{L}\right)^{-1}. \quad (1.2)$$

A more complex distribution containing four free parameters makes up the Epstein layer [3]:

$$\frac{\varepsilon(z)}{\varepsilon(z=0)} = 1 - \frac{Nf}{1+f} - \frac{4Mf}{(1+f)^2},$$

$$f = \exp[a(z+z_1)]. \quad (1.3)$$

A comprehensive analysis of the models (1.1)–(1.3), which describe media with a moderate natural dispersion of the wave velocity, was performed in the monograph [4] concerned with the problems of acoustics of stratified media.

In contrast to the models (1.1)–(1.3), the distributions (1.4) and (1.5) correspond to plasma-like dielectrics with the frequency dispersion

$$\varepsilon(z) = 1 - g(\omega)W(z). \quad (1.4)$$

Here, the $g(\omega)$ factor depends on the wave frequency and the parameters of the dielectric, while the dimensionless function W defines the electron distribution. Exact solutions of the Maxwell equations are known for linear [5], parabolic [6], and exponential [7] profiles of the normalized density W :

$$W = 1 + \frac{z}{L}; \quad W = 1 - \frac{z^2}{L^2}; \quad W = \exp\left(\frac{z}{L}\right). \quad (1.5)$$

When it comes to nonlocal dispersion, it is pertinent to note that this review is devoted to dispersion effects related to macroscopic medium-nonuniformity scale lengths L ; in this case, the ratio between the wavelength λ in vacuum and the quantity L may be arbitrary. It is not our intention to discuss here the widely known effects of spatial dispersion [8] determined by a microscopic medium inhomogeneity at distances of the order of a , where a is the size of molecules or the lattice spacing ($a \ll \lambda$).

Since only a limited number of stratified media models are exactly solvable, investigators' attention is drawn to approximate methods employed, for instance, in geometrical optics [9, 10] and to the numerical simulation of wave problems, which now forms the basis of the special course of studies entitled "Computer Electromagnetics" in many universities in Europe and the USA. Numerical techniques increase in importance still further when we turn to the optics of nonstationary media, where analytical results are seldom the case. The limiting cases of adiabatic oscillations and rapid jump-like variations of $\varepsilon(t)$ are described in Refs [11, 12]. Examples of amplitude-phase evolution of near-breakdown fields in a plasma are illustrated numerically in Refs [13, 14]. Exact solutions for the fast dispersion distortion of short video pulses in nonuniform dielectrics were found in Ref. [15].

The time-dependent diffraction of such pulses was considered analytically in Refs [16, 17].

An analysis of these results suggests that the spatiotemporal envelopes of the electric and magnetic components \mathbf{E} and \mathbf{H} of the wave field propagating through a layered or nonstationary medium suffer complex distortions. In particular, when a wave with harmonic envelopes of \mathbf{E} and \mathbf{H} is incident on the surface of a stratified medium, the shape of the spatial envelope of \mathbf{E} within the medium becomes nonsinusoidal and changes during the propagation. Simultaneously distorted is the spatial envelope of \mathbf{H} , whose shape can significantly differ from that of \mathbf{E} . The rate of this distortion is determined by the nonlocal dispersion of the medium. Similar effects also develop in the time envelopes of E and H in a nonstationary medium.

Therefore, a new branch of the wave theory — the optics of nonsinusoidal waves — is formed in studies of electromagnetic fields in stratified and nonstationary media. Several 'burning' problems which are of consequence for the development of this new avenue of investigation are discussed below.

1. Construction of exact analytical solutions of the Maxwell equations for strato-nonuniform (one-dimensionally nonuniform) dielectrics. To find such solutions, we systematically employ special transformations of the Maxwell equations which eliminate the explicit dependence of these equations on the $\varepsilon(z)$ distribution: in this case, the spatial field structure at a point z within the medium depends on the phase path $\eta(z)$ traversed by the wave from the medium boundary to the point z (η is the phase coordinate). The conditions of such a transformation define broad classes of continuous $\varepsilon(z)$ distributions allowing exact analytical representations for the electromagnetic field components. The flexibility of such models, which represent both monotonic and modulated profiles of $\varepsilon(z)$ with an arbitrary modulation depth and shape, is characterized by the existence of several free parameters. The spatial field structure in the new variables — the phase coordinates η — is in some cases represented by elementary functions (see Sections 2, 5, and 6).

Several previously known, exactly solvable models of $\varepsilon(z)$ for nonuniform dielectrics prove to be special cases of the multiparameter $\varepsilon(z)$ distributions derived here.

2. Strong nonlocal dispersion of electromagnetic waves in stratified dielectrics. Employing exactly solvable models of $\varepsilon(z)$ permits the dispersion of nonuniform dielectrics to be represented by waveguide-type formulas. The characteristic frequencies in these formulas are determined by the nonuniformity scale of $\varepsilon(z)$; the nonlocal dispersion can be either normal or anomalous, depending on the $\varepsilon(z)$ profile. The cutoff frequency for a stratified dielectric, which is determined by the $\varepsilon(z)$ profile, may occur in a spectral region far from the resonance frequencies and the absorption bands of the material (see Section 2).

For special $\varepsilon(z)$ profiles characterized by the absence of nonlocal dispersion, the geometrical optics approximation yields an exact solution of the wave equation (see Section 3).

3. Effects of broadband reflection and transmission of radiation in nonuniform media. The nonlocal dispersion of a nonuniform dielectric layer can radically change the reflection properties of the dielectric. Broad spectral intervals of reflectionless transmission and strong reflection of radiation, determined by the $\varepsilon(z)$ profile, arise in such a layer. The compensation of phase shifts which appear as a wave passes through a nonuniform dielectric and a dissipative medium

permits the optimization of the parameters of broadband reflectionless coatings for absorbing materials (see Sections 4 and 7). Advantage is taken of the phase coordinates to consider the propagation of electromagnetic waves through a plasma with a modulated density for symmetric and asymmetric density profiles and an arbitrary modulation depth (see Sections 5 and 6).

The importance of the gradient and the curvature of the $\varepsilon(z)$ profile for the formation of broadband reflectionless properties of dielectrics was demonstrated with the aid of the generalized Fresnel formulas.

4. Dispersion of nonstationary media with a finite relaxation time. The exactly solvable models of nonuniform dielectrics, considered above, are generalized to the case of a time-dependent permittivity $\varepsilon(t)$. The dispersion of such dielectrics is described by waveguide-type formulas with characteristic frequencies determined by the relaxation times of $\varepsilon(t)$. Exact analytical solutions of the Maxwell equations describe nonsinusoidal waves in such media. We note the feasibility of total wave reflection from a nonstationary dielectric for certain relationships between the wave frequency and the relaxation times of $\varepsilon(t)$ (see Section 8). The effect of relaxation time on the reflection properties of a conductor is demonstrated based on an exactly solvable model for the telegraph equation with a time-dependent conductivity $\sigma(t)$ (see Section 9).

A generalized model is constructed on the basis of the Fresnel formulas for nonstationary dielectrics, which describes the dynamic effects of the first and second derivatives of the $\varepsilon(t)$ dependence on the amplitude oscillations and on the broadening of the spectrum of the reflected wave.

5. Application of methods of the optics of stratified media to the allied domains of the wave theory. We consider examples of how the above mathematical formalism is applied to the theory of long transmission lines with continuously distributed parameters, nonlinear optics, magneto-optics, and quantum mechanics. Ways are highlighted toward broadening the class of transformations of the Maxwell equations in a continuous medium that lead to new exactly solvable models of $\varepsilon(z)$ (see Section 10). We point out the prospects of harnessing the optics of stratified and nonstationary media for conducting prompt tests of the parameters of optoelectronics materials.

2. Nonlocal dispersion of stratified media. Phase coordinate method

This section is dedicated to the construction of a mathematical scheme of describing large-scale dispersion effects in stratified media. Let us consider the propagation of a plane wave in a nonuniform, nonmagnetic dielectric whose permittivity ε depends on the z -coordinate. To distinguish the effects associated with the nonuniformity of ε , we assume that the wave absorption and the material dispersion are insignificant in the range of frequencies ω under consideration. In this case, the $\varepsilon(z)$ dependence in the transparency region ($\varepsilon > 0$) can be represented as

$$\varepsilon(z) = n_0^2 U^2(z), \quad U \Big|_{z=0} = 1. \quad (2.1)$$

Here, n_0 is the refractive index of the medium at the boundary $z = 0$ and the dimensionless function U^2 describes the spatial permittivity distribution.

The Maxwell equations for a linearly polarized wave with components E_x and H_y , which travels in the z -direction through a medium obeying expressions (2.1), are of the form

$$\frac{\partial E_x}{\partial z} = -\frac{1}{c} \frac{\partial H_y}{\partial t}, \quad (2.2)$$

$$-\frac{\partial H_y}{\partial z} = \frac{n_0^2 U^2(z)}{c} \frac{\partial E_x}{\partial t}. \quad (2.3)$$

The function $U^2(z)$ still remains unknown.

Unlike the exactly solvable models (1.1)–(1.5) pointed out in the Introduction, new analytical solutions of the system (2.2), (2.3) will be derived employing a special transformation in the space of phase trajectories. This approach leads to several new, exactly solvable models for $\varepsilon(z)$ and allows a clear representation of strong dispersion effects arising from the permittivity profile. Expressing the E_x and H_y components of the wave field in terms of some auxiliary function ψ permits the system of first-order equations (2.2), (2.3) to be reduced to one second-order equation for the ψ function. This transformation can be accomplished in two different ways:

(1) the auxiliary function ψ is selected so that Eqn (2.2) becomes an identity while the ψ function itself is defined by Eqn (2.3);

(2) the ψ function that makes Eqn (2.3) an identity is determined from Eqn (2.2).

It is appropriate to consider separately the solutions constructed in these ways.

1. We express the wave field components in terms of a vector potential \mathbf{A} :

$$\mathbf{E} = -\frac{1}{c} \frac{\partial \mathbf{A}}{\partial t}, \quad \mathbf{H} = \text{rot } \mathbf{A}. \quad (2.4)$$

In the geometry of the problem (2.2), (2.3) under study, the vector potential has only one component A_x ($A_y = A_z = 0$). Expressing the A_x component in terms of the normalizing constant A_0 and the dimensionless function $\psi(z, t)$ permits Eqn (2.3), which determines the function ψ , to be written as

$$\frac{\partial^2 \psi}{\partial z^2} - \frac{n_0^2 U^2(z)}{c^2} \frac{\partial^2 \psi}{\partial t^2} = 0. \quad (2.5)$$

One can see from Eqn (2.5) that the unknown function ψ obeys a wave equation with a coordinate-dependent velocity of wave propagation.

Eqn (2.5) can be conveniently solved by introducing new functions F and Q and a new variable η [18]:

$$\psi = \frac{F}{\sqrt{U}}; \quad Q = U^{-1}; \quad \eta = \int_0^z U(z_1) dz_1. \quad (2.6)$$

In this case, Eqn (2.5) rearranges to the form

$$\frac{\partial^2 F}{\partial \eta^2} - \frac{n_0^2}{c^2} \frac{\partial^2 F}{\partial t^2} = F \left[\frac{1}{2} Q \frac{\partial^2 Q}{\partial z^2} - \frac{1}{4} \left(\frac{\partial Q}{\partial z} \right)^2 \right]. \quad (2.7)$$

The function $Q(z)$ still remains unknown.

Consider, for instance, a simple particular solution of Eqn (2.7) which corresponds to the function Q defined by the conditions

$$\frac{1}{2} Q \frac{\partial^2 Q}{\partial z^2} - \frac{1}{4} \left(\frac{\partial Q}{\partial z} \right)^2 = p^2. \quad (2.8)$$

Here, p^2 is some constant which will be defined below. Assuming that the time dependence of the field F is harmonic, Eqn (2.7) can be written, in view of expression (2.8), as

$$\frac{\partial^2 F}{\partial \eta^2} + \left(\frac{n_0^2 \omega^2}{c^2} - p^2 \right) F = 0. \quad (2.9)$$

Note that the η -coordinate (2.6) is proportional to the phase path L_p in the nonuniform medium: $L_p = n_0 \eta$. Eqn (2.9) describes a sinusoidal wave traveling in the η -direction:

$$F \sim \exp[i(q\eta - \omega t)].$$

We substitute this expression for the function F into Eqn (2.9) to represent the dimensionless vector potential ψ as a traveling wave with a spatially modulated amplitude:

$$\psi = \frac{\exp[i(q\eta - \omega t)]}{\sqrt{U(z)}},$$

$$q = kN; \quad k = \frac{\omega n_0}{c}; \quad N = \sqrt{1 - \frac{\Omega^2}{\omega^2}}; \quad \Omega^2 = \frac{p^2 c^2}{n_0^2}. \quad (2.10)$$

The factor N (2.10) for $p^2 > 0$ is similar to the refractive index for the waves propagating in a waveguide with a cutoff frequency Ω . To calculate the electromagnetic field components E_x and E_y from (2.10), the function $Q = U^{-1}$ should be found from Eqn (2.8), the parameter p^2 should be determined, and the η -variable should be expressed in terms of the z -coordinate. The profile $U(z)$ that allows a representation of the field ψ in the form (2.10) is given by the solution of Eqn (2.8):

$$U(z) = \left(1 + s_1 \frac{z}{L_1} + s_2 \frac{z^2}{L_2^2} \right)^{-1},$$

$$s_1 = 0, \pm 1, \quad s_2 = 0, \pm 1. \quad (2.11)$$

Here, L_1 and L_2 are the free parameters of the model (2.11), which have the meaning of characteristic nonuniformity scale lengths for the permittivity. The distributions (2.11) are shown in Fig. 1. If s_1 and s_2 are of the same sign, the dependences $U(z)$ are monotonic; when s_1 and s_2 are of different sign, there appear extrema of the functions $U(z)$:

$$U_{\max} = (1 - y^2)^{-1}; \quad U_{\min} = (1 + y^2)^{-1}; \quad y = \frac{L_2}{2L_1}. \quad (2.12)$$

In the limiting case $L_2 \rightarrow \infty$ the function (2.11) corresponds to the profile (1.1) for which the exact solution was pointed out by Rayleigh [1].

We substitute formula (2.11) into (2.8) to obtain the following expression for the parameter p^2 :

$$p^2 = \frac{s_1^2}{4L_1^2} - \frac{s_2}{L_2^2}. \quad (2.13)$$

Depending on the ratio between the characteristic lengths L_1 and L_2 and the signs of s_1 and s_2 , the parameter p^2 can assume positive, negative, or zero values. In each of these cases, the η -variable (2.6) is represented by different formulas. For

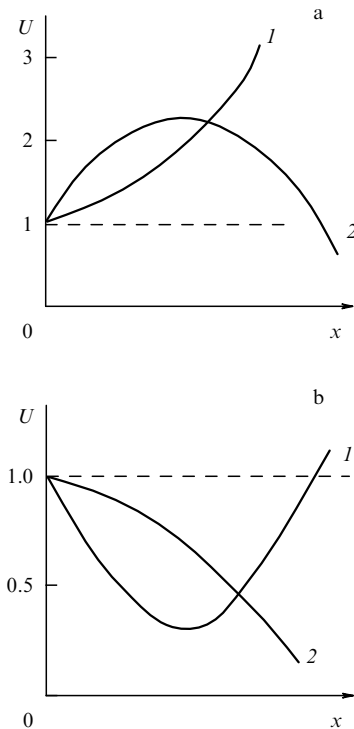


Figure 1. Exactly solvable models of the spatial profiles of the normalized permittivity U (2.11), $x = zL_1^{-1}$: (a) curve 1 corresponds to the case $s_1 = -1$, $s_2 = +1$, whereas the signs of s are similar for curve 2: $s_1 = s_2 = -1$; (b) curve 1 corresponds to the case $s_1 = +1$, $s_2 = -1$ and curve 2, to the case $s_1 = s_2 = +1$.

instance,

$$\eta \Big|_{p^2 > 0, s_2 < 0} = \frac{L_2}{\sqrt{1 + y^2}} \operatorname{artanh} \frac{zL_2^{-1} \sqrt{1 + y^2}}{1 + s_1 z / 2L_1}, \quad (2.14)$$

$$\eta \Big|_{p^2 > 0, s_2 > 0} = \frac{L_2}{\sqrt{y^2 - 1}} \operatorname{artanh} \frac{zL_2^{-1} \sqrt{y^2 - 1}}{1 + s_1 z / 2L_1}, \quad y^2 > 1, \quad (2.15)$$

$$\eta \Big|_{p^2 < 0, s_2 > 0} = \frac{L_2}{\sqrt{1 - y^2}} \arctan \frac{zL_2^{-1} \sqrt{1 - y^2}}{1 + s_1 z / 2L_1}, \quad y^2 < 1. \quad (2.16)$$

In the limit $L_2 \rightarrow \infty$, the η -variable is of the form

$$\eta = L_1 \ln \left(1 + \frac{z}{2L_1} \right).$$

The case $p^2 = 0$ is considered below. All the quantities that determine the vector potential ψ (2.10) are now expressed in terms of the nonuniformity parameters.

Our results permit the effect of nonlocal dispersion of a nonuniform dielectric (2.11) to be revealed. This effect, determined by the parameters L_1 , L_2 , s_1 , and s_2 of the profile $U(z)$, is described by the factor N (2.10). For $p^2 > 0$, the medium is characterized by a normal dispersion

$$N = \sqrt{1 - \frac{\Omega_1^2}{\omega^2}}, \quad \Omega_1^2 = \frac{c^2(1 + y^2)}{n_0^2 L_2^2}. \quad (2.17)$$

Otherwise ($p^2 < 0$), the permittivity nonuniformity is responsible for an anomalous dispersion:

$$N = \sqrt{1 + \frac{\Omega_2^2}{\omega^2}}, \quad \Omega_2^2 = \frac{c^2(1 - y^2)}{n_0^2 L_2^2}. \quad (2.18)$$

We emphasize that the resultant characteristic frequencies Ω_1 and Ω_2 are controlled by the nonuniformity parameters alone and are not related to the material dispersion. The effect of the characteristic frequencies Ω_2 and Ω_2 on the wave reflection from a nonuniform dielectric is discussed in Sections 4 and 5.

Therefore, solving Eqns (2.2) and (2.3) through the first procedure permitted the field in a nonuniform dielectric (2.11) to be represented as modulated traveling waves. Before discussing the properties of such fields, there is good reason to dwell on other exactly solvable nonuniformity profiles in dielectrics described in the context of the second procedure.

2. Unlike representation (2.4), the system (2.2), (2.3) can be reduced to one equation by introducing an unknown function Θ according to the formulas [19]

$$E_x = \frac{B_0}{U^2(z)} \frac{\partial \Theta}{\partial z}, \quad H_y = -\frac{B_0 n_0^2}{c} \frac{\partial \Theta}{\partial t}. \quad (2.19)$$

Here, B_0 is the normalizing constant. Upon substitution of formulas (2.19) into the system (2.2), (2.3), Eqn (2.3) becomes an identity while the function Θ is defined by the equation following from Eqn (2.2):

$$\frac{\partial^2 \Theta}{\partial z^2} - \frac{n_0^2 U^2(z)}{c^2} \frac{\partial^2 \Theta}{\partial t^2} = \frac{2}{U} \frac{\partial U}{\partial z} \frac{\partial \Theta}{\partial z}. \quad (2.20)$$

Eqn (2.20) can be solved through the same procedure as Eqn (2.5). We introduce new functions f and Q and use the η -variable (2.6):

$$\Theta = f\sqrt{U}, \quad Q = U^{-1/2}. \quad (2.21)$$

In view of expressions (2.21), Eqn (2.20) can be rearranged to give

$$\frac{\partial^2 f}{\partial \eta^2} - \frac{n_0^2}{c^2} \frac{\partial^2 f}{\partial t^2} = \frac{f}{Q} \frac{\partial^2 Q}{\partial \eta^2}. \quad (2.22)$$

We consider the nonuniformity profiles satisfying the condition

$$\frac{\partial^2 Q}{\partial \eta^2} = p^2 Q, \quad (2.23)$$

where p^2 is some constant. Depending on the sign of this constant, the distributions of $U = Q^{-2}$ described by Eqn (2.23) can be represented as

$$U \Big|_{p^2 > 0} = [\cosh(p\eta) + M \sinh(p\eta)]^{-2}, \quad p^2 > 0, \quad (2.24)$$

$$U \Big|_{p^2 < 0} = [\cos(p_1\eta) + M_1 \sin(p_1\eta)]^{-2}, \quad p_1^2 = -p^2 > 0. \quad (2.25)$$

The constants M and p^2 are determined by the parameters of the $U(z)$ profile. The case $p^2 = 0$ is treated separately.

When the condition (2.23) is fulfilled, the function f (2.22) is represented by a traveling wave in the variables η and t ,

while the solution of Eqn (2.20) takes the form of a spatially modulated wave

$$\Theta = \sqrt{U(z)} \exp[i(q\eta - \omega t)]. \quad (2.26)$$

The wave number q in expression (2.26) was defined in (2.10); however, the profile $U(z)$, the parameter p^2 , and the η -variable should be calculated anew. This consideration can be conveniently performed separately for the cases $p^2 > 0$ and $p^2 < 0$. We introduce the characteristic nonuniformity scale length

$$L = |p|^{-1} \quad (2.27)$$

and consider the following two cases.

Case 1: $p^2 > 0$. Solving expression (2.24) for the η -variable and comparing it with its definition (2.6), we arrive at an equation for the profile $U(z)$:

$$\frac{\partial U}{\partial z} = \pm \frac{2U^2}{L} \sqrt{1 - U(1 - M^2)}, \quad 0 \leq M \leq 1. \quad (2.28)$$

The plus and minus signs in the right-hand side of Eqn (2.28) correspond to the ascending and descending $U(z)$ dependences, respectively. By solving this equation with the plus sign, it is possible to investigate the growth of the dimensionless function U from the value $U = 1$ at the boundary of the medium to the maximum value $U_{\max} = (1 - M^2)^{-1}$:

$$\frac{z}{L} = \frac{1}{2} \left[M - \frac{\sqrt{1 - U(1 - M^2)}}{U} + (1 - M^2) \operatorname{artanh} \frac{U - 1}{\sqrt{1 - U(1 - M^2)} + MU} \right]. \quad (2.29)$$

The distance from the boundary to the point at which a maximum U_{\max} is attained, z_m , is as follows:

$$\frac{z_m}{L} = \frac{1}{2} \left[M - (1 - M^2) \operatorname{artanh} M \right]. \quad (2.30)$$

After the peak ($z \geq z_m$), the nonuniformity profile U is determined by the descending branch of the solution of Eqn (2.28), which corresponds to the minus sign in the right-hand side of this equation:

$$\frac{z - z_m}{L_2} = \frac{1}{2} \left[\frac{\sqrt{1 - U(1 - M^2)}}{U} + (1 - M^2) \operatorname{artanh} \sqrt{1 - U(1 - M^2)} \right]. \quad (2.31)$$

This solution describes a decrease of U from $U = U_{\max}$ to $U = 1$.

The dependences (2.24) and (2.31) characterize the family of $U(z)$ profiles with two free parameters M and L (Fig. 2a). Unlike the explicit expression for the function $U(z)$ (2.11) obtained in the context of the first procedure, the profile (2.29) is expressed through the inverse function $z = z(U)$. This function is, together with its first derivative, continuous at the maximum z_m , where both branches are tangential to one another. It is significant that this continuity is retained even when the values of the parameters L and L_2 , which characterize the branches (2.29) and (2.31), are different; if so, the cases where $L = L_2$ and $L \neq L_2$ correspond to $U(z)$

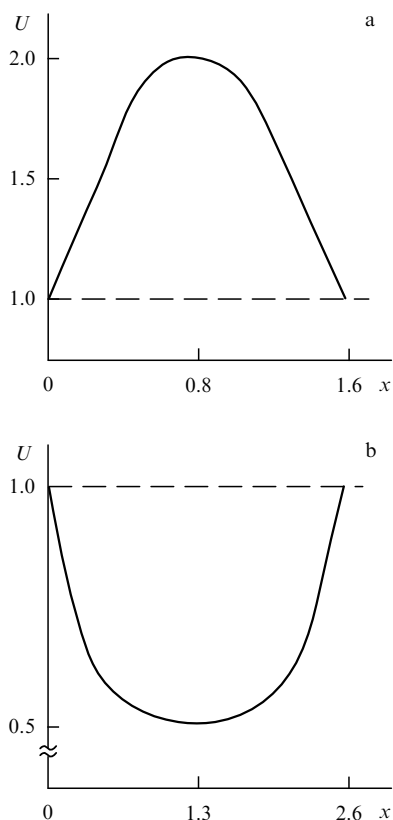


Figure 2. $U(x)$ dependences, $x = zL^{-1}$: (a) in the model (2.29), $M = 0.7$; (b) in the model (2.33), $M = 0.5$.

profiles symmetric and asymmetric about the maximum U_{\max} , respectively.

Case 2: $p^2 < 0$, $p^2 = -p_1^2$, $L_1 = |p_1|^{-1}$. The analysis is performed according to the same procedure as in the case where $p^2 > 0$. Taking advantage of relationship (2.25), it is possible to write down the differential equation for $U(z)$:

$$\frac{\partial U}{\partial z} = \pm \frac{2U^2}{L_1} \sqrt{U(1 + M_1^2) - 1}. \quad (2.32)$$

The descending and ascending branches of the solution of Eqn (2.32), which determine the decrease of the function U from $U = 1$ to the minimum $U(z_1) = (1 + M_1^2)^{-1}$ and the subsequent growth of U from the minimum to the value $U(z = z_3) = 1$, are described by the solutions of Eqn (2.32):

$$\begin{aligned} \frac{z}{L_1} &= \frac{1}{2} \left[M_1 - \frac{\sqrt{U(1 + M_1^2) - 1}}{U} \right. \\ &\quad \left. + (1 + M_1^2) \arctan \frac{1 - U}{\sqrt{U(1 + M_1^2) - 1} + M_1 U} \right], \\ \frac{z - z_1}{L_3} &= \frac{1}{2} \left[\frac{\sqrt{U(1 + M_1^2) - 1}}{U} \right. \\ &\quad \left. + (1 + M_1^2) \arctan \sqrt{U(1 + M_1^2) - 1} \right]. \quad (2.33) \end{aligned}$$

The rise and fall of the function U are shown in Fig. 2b.

Now let us find the phase path η (2.6) for the profiles (2.30) and (2.33). Since the $U(z)$ dependence is prescribed with the aid of inverse functions $z = z(U)$, it is advantageous to make use of the differential expression for η in the form $d\eta = U dz$. We substitute the value of dz from Eqn (2.28) and rewrite formula (2.6) as

$$\eta = \frac{L}{2} \int_1^U \frac{dU_1}{U_1 \sqrt{1 - U_1(1 - M^2)}}. \quad (2.34)$$

We calculate the integral (2.34) to obtain

$$\eta = \frac{L}{2} \ln \frac{\tan[(1/2) \arcsin \sqrt{U(1 - M^2)}]}{\tan[(1/2) \arcsin \sqrt{1 - M^2}]}. \quad (2.35)$$

The phase path for the profile (2.33) is found in a similar way:

$$\begin{aligned} \eta &= 2L \left[\arctan(M + \sqrt{1 + M^2}) \right. \\ &\quad \left. - \arctan\left(\sqrt{U(1 + M^2)} + \sqrt{U(1 + M^2) - 1}\right) \right]. \quad (2.36) \end{aligned}$$

Therefore, the field in nonuniform dielectrics, which are characterized by the $z(U)$ profiles prescribed with the aid of the inverse functions (2.30) and (2.33), is also represented as a traveling wave (2.26) in the space of phase trajectories. The nonlocal dispersion of such media, caused by the nonuniformity of $\varepsilon(z)$, is described by the parameter N (2.10). The normal and anomalous dispersions are determined by formulas (2.17) and (2.18), the characteristic frequencies corresponding to the profiles (2.30) and (2.33):

$$\Omega_1^2 = \frac{c^2}{n_0^2 L^2}, \quad \Omega_2^2 = \frac{c^2}{n_0^2 L_1^2}. \quad (2.37)$$

Despite the fact that the formulas describing the nonuniform dielectric models (2.11) and (2.29) are different, several common properties of these models are noteworthy.

1. In the determination of the wave number $q = \omega n_0 c^{-1} N$ (2.10), the local frequency dispersion of the refractive index $n_0(\omega)$ is not taken into account. The dispersion-induced variation in the wave number Δq corresponding to a frequency shift $\Delta \omega$ is given by the relationship

$$\Delta q q^{-1} = \Delta \omega n_0^{-1} \frac{\partial n_0}{\partial \omega}.$$

Away from the resonance frequencies this ratio is small: $\Delta q q^{-1} \lesssim 10^{-2}$. At the same time, the nonlocal dispersion characterized by the frequencies $\Omega_{1,2}$ can radically alter not only the magnitude of q , but the very nature of propagation, for instance, for frequencies $\omega < \Omega_1$.

2. In the analysis of the models (2.11) and (2.29), it was assumed that the nonuniformity distribution scale length L is far shorter than the characteristic absorption lengths; in this case, the absorption was neglected and the values of L were real. However, these same models are easily generalized to the case of an absorbing dielectric with a nonuniform distribution of complex permittivity. In this case, the parameters L_1 and L_2 are complex quantities: $L = \text{Re } L + i \text{Im } L$.

3. The traveling waves (2.10) describe only one of the solutions of Eqn (2.9) — the direct wave. The second solution of this equation (the return wave) corresponds to the replacement of the factor $\exp(iq\eta)$ with $\exp(-iq\eta)$ in the solution (2.10).

3. When does the WKB approximation yield exact solutions of the wave equation?

The solution of a one-dimensional wave equation for a medium with the coordinate-dependent refractive index (2.10) provides a traditional example of constructing approximate solutions within the framework of the WKB method [9]. This method, based on the assumption that the refractive index varies only slightly over a distance of a wavelength, permits the approximate solution of Eqn (2.10) to be written as

$$\psi = [U(z)]^{-1/2} \exp \left[i \left(k \int U dz - \omega t \right) \right], \quad k = \frac{\omega n_0}{c}. \quad (3.1)$$

By comparing expression (3.1) with the exact solution (2.10), it can easily be found that these solutions coincide when $k = q = \omega n_0 N c^{-1}$. In other words, the solution (3.1) is exact when the parameter N (2.10) is equal to unity, i.e.,

$$p = 0. \quad (3.2)$$

As seen from the definition of the quantity p^2 (2.13), the characteristic nonuniformity scale lengths L_1 and L_2 in this case are related as $L_2 = 2L_1$. The profile of $\varepsilon(z)$ corresponding to the equality (3.2) is determined by expression (2.11):

$$\varepsilon(z) = n_0^2 \left(1 + \frac{s_1 z}{2L_1} \right)^{-4}. \quad (3.3)$$

The η -coordinate (2.6) for the profile (3.3) is given by the expression

$$\eta = z \left(1 + \frac{s_1 z}{2L_1} \right)^{-1}. \quad (3.4)$$

The solution (3.1) corresponds to the WKB approximation for Eqn (2.5), which originates when the Maxwell equations (2.2), (2.3) are transformed with the aid of the function ψ (2.4). Transforming the same equations with the aid of the function Θ (2.19) leads to Eqn (2.20). The approximate solution of Eqn (2.20) obtained within the framework of the WKB approximation is of the form

$$\Theta = \sqrt{U(z)} \exp \left[i \left(k \int U dz - \omega t \right) \right]. \quad (3.5)$$

By analogy with the case (3.1), it can be shown that expression (3.5) is an exact solution of Eqn (2.5) if the condition $p = 0$ (3.2) is fulfilled. The permittivity profile and the phase path η can be found from Eqns (2.21) and (2.23):

$$\varepsilon(z) = n_0^2 \left(1 + \frac{z}{L} \right)^{-4/3}, \quad (3.6)$$

$$\eta = 3L \left[\left(1 + \frac{z}{L} \right)^{1/3} - 1 \right]. \quad (3.7)$$

The resultant expressions (3.3) and (3.6) describe the permittivity profiles for which the WKB approximations coincide with the exact solutions. On the strength of condition (3.2), the nonlocal dispersion does not occur for waves propagating in these media.

Therefore, the WKB approximations for the field equations (2.5) and (2.20) can be regarded as special cases of the general solutions derived by transforming the Maxwell equations (2.2), (2.3) in the space of phase trajectories $\eta = \eta(z)$. In other words, in the absence of artificial dispersion of the nonuniform layer ($p = 0$), the nonuniformity causes the amplitude and the phase of the field to change, but the wave number q remains invariable during propagation. A similar effect is considered in Section 8 also for nonstationary media: for a certain time dependence of the permittivity (8.40), the wavelength of the radiation propagating through this medium does not vary.

4. Broadband reflectionless properties of nonuniform dielectric layers

It was noted in Section 2 that the permittivity distributions (2.11) and (2.29) are convenient for the description of optically nonuniform layers of finite thickness and thin films in particular. Such films deposited on a surface are widely used to alter the reflectivity of this surface. Owing to the interference of the waves reflected from the surface and from the film coating, the reflected waves may quench each other. This situation arises, for instance, when a wave is incident normally from the air onto a film of thickness d , which covers a half-space with a refractive index n_1 . If the quantities d and n_1 , the wavelength λ , and the refractive index of the film material n_0 are related as

$$n_1 = n_0^2; \quad \lambda_m = \frac{4n_0 d}{m}, \quad m = 1, 2, 3, \dots, \quad (4.1)$$

then, as is well known [23], all the waves enter the film-coated half-space without reflection (a 'quarter-wave' plate). However, this resonance effect arises in a uniform layer only for a discrete wavelength spectrum (4.1). Nonuniform dielectric layers with a special permittivity profile $\varepsilon(z)$ hold promise for the formation of broadband reflectionless coatings. Techniques for producing such coatings on the basis of polymers [20], ZnSe-type semiconductor materials [21] and silicon nitrides [22] have been elaborated in recent years.

To optimize the reflection properties of a nonuniform layer over a broad frequency range, advantage can be taken of the artificial dispersion effects (see Section 2). We consider a plate of thickness d with a refractive index profile $n(z) = n_0 U(z)$, which covers the surface of an optically uniform material with a complex refractive index $n_2 + i\kappa_2$ (Fig. 3); the dimensionless function $U(z)$ is assumed to be of the form (2.11). Let us assume that a wave with a frequency ω is incident normally from the air onto a plate surface $z = 0$. For the $U(z)$ profile (2.11), the electric (E_x) and magnetic (H_y) components of the wave field in the plate material ($0 \leq z \leq d$) can be determined by substitution of the vector potential (2.10) into formulas (2.4):

$$\begin{aligned} E_x &= iA_1 \omega c^{-1} U^{-1/2} \exp[i(q\eta - \omega t)], \\ H_y &= iA_1 \omega n_0 c^{-1} U^{1/2} (N - iG) \exp[i(q\eta - \omega t)], \end{aligned} \quad (4.2)$$

$$G = \frac{c}{2\omega n_0} \left(\frac{s_1}{L_1} + \frac{2s_2 z}{L_2^2} \right). \quad (4.3)$$

Here, A_1 is the normalizing constant; the value of the quantity N is given by formula (2.10); n_0 , $L_{1,2}$, and $s_{1,2}$ are the parameters of the model (2.11).

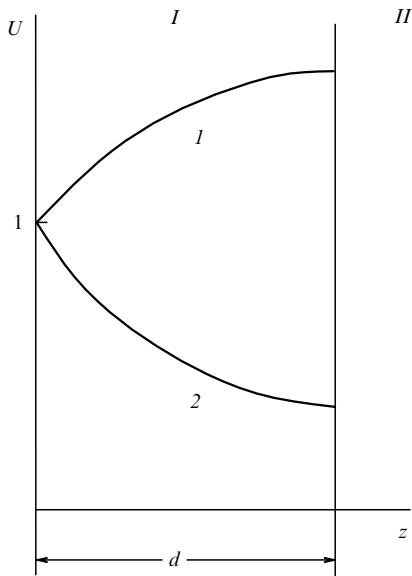


Figure 3. Transition layer *I* of a nonuniform dielectric of thickness *d* on the surface of a uniform absorbing dielectric *II*. Curves 1 and 2 correspond to the cases of normal and anomalous nonlocal dispersion in the model $U(z)$ (2.11).

The total field within the plate, derived with the inclusion of the wave reflected by the surface $z = d$, can be written as

$$E_x = i\omega A_1 c^{-1} U^{-1/2} [\exp(iq\eta) + K \exp(-iq\eta)] \exp(-i\omega t), \tag{4.4}$$

$$H_y = i\omega A_1 n_0 c^{-1} U^{1/2} \left\{ N [\exp(iq\eta) - K \exp(-iq\eta)] - iG [\exp(iq\eta) + K \exp(-iq\eta)] \right\} \exp(-i\omega t). \tag{4.5}$$

Expressions (4.4) and (4.5) imply that the amplitudes of the direct and reflected waves are equal, respectively, to unity and K . The components of the wave field in the air ($z \leq 0$) can be written by introducing the electric-field reflectivity R [23]:

$$\begin{aligned} E_x &= i\omega A_0 c^{-1} [\exp(ikz) + R \exp(-ikz)] \exp(-i\omega t), \\ H_y &= i\omega A_0 c^{-1} [\exp(ikz) - R \exp(-ikz)] \exp(-i\omega t), \\ k &= \omega c^{-1}. \end{aligned} \tag{4.6}$$

Substituting expressions (4.4)–(4.6) into the conditions for continuity of the electric and magnetic field components at the boundary $z = 0$ ($\eta = 0$) permits the quantity R to be represented as

$$R = \frac{1 - B}{1 + B}, \quad B = n_0 \left[N \left(\frac{1 - K}{1 + K} \right) - iG_0 \right]. \tag{4.7}$$

The parameter G_0 in expressions (4.7) is related to the parameter G in formula (4.3):

$$G_0 = G \Big|_{z=0} = \frac{cs_1}{2\omega n_0 L_1}. \tag{4.8}$$

The formula for the reflectivity R (4.7) contains an unknown quantity K , which can be calculated from the conditions for continuity of E_x and H_y at the boundary $z = d$. By substituting the vector potential of the traveling

wave in the $z \geq d$ domain as

$$A_2 \exp[i(n_2 + i\alpha_2)(z - d) - i\omega t],$$

it is possible to find the value of K :

$$K = -\frac{n_2 + i\alpha_2 + P_1}{n_2 + i\alpha_2 - P_1} \exp(2iq\eta_1), \tag{4.9}$$

$$\eta_1 = \eta(d), \quad U_1 = U(d), \quad G_1 = G(d),$$

$$P_1 = n_0 U_1 (N - iG_1). \tag{4.10}$$

Upon substitution of K (4.9) into the formula that defines B (4.7), we separate the real and imaginary parts of this expression:

$$B = \text{Re } B + i \text{Im } B, \tag{4.11}$$

$$\text{Re } B = [n_0^2 N^2 U_1 (1 + t^2)] n_2 \Delta^{-1}, \quad t = \tan(q\eta_1), \tag{4.12}$$

$$\Delta = n_2 t^2 + [\alpha_2 t + n_0 U_1 (N + G_1 t)]^2, \tag{4.13}$$

$$\begin{aligned} \text{Im } B &= n_0 N \Delta^{-1} \left\{ t + n_2^{-2} [\alpha_2 + n_0 U_1 (G_1 - Nt)] \right. \\ &\quad \left. \times [\alpha_2 t + n_0 U_1 (N + G_1 t)] \right\} - n_0 G_0. \end{aligned} \tag{4.14}$$

With a knowledge of the values of $\text{Re } B$ (4.12) and $\text{Im } B$ (4.14), it is possible to derive the complex reflectivity R from expressions (4.7).

The amplitude and phase of the R coefficient essentially depend on the characteristic nonuniformity scale lengths L_1 and L_2 as well as on the values of s_1 and s_2 .

This dependence manifests itself, in particular, in the influence of the artificial frequency dispersion (2.17), (2.18) on the reflection processes. This effect can easily be illustrated by the example of a simplified problem of reflection from a nonuniform transparent plate in the air ($n_2 = 1, \alpha_2 = 0$). The effects of normal ($p^2 > 0$) and anomalous ($p^2 < 0$) artificial dispersion are treated below separately.

1. $p^2 > 0$. In this case, which corresponds to the upper curve in Fig. 3, the medium is characterized by the cutoff frequency Ω_1 (2.17). By introducing the normalized wave frequency $x_1 = \omega \Omega_1^{-1}$, it is possible to write the expression for the parameter t (4.13) as

$$\begin{aligned} t &= \tan \left(\sqrt{x_1^2 - 1} \operatorname{artanh} u_1 \right), \\ u_1 &= \left(dL_2^{-1} \sqrt{1 + y^2} \right) (1 + ydL_2^{-1})^{-1}. \end{aligned} \tag{4.15}$$

From this point on, d is the layer thickness, and the values $x_1 > 1$ correspond to the transparent region. The frequency dependence of the reflectivity for $\omega > \Omega_1$ is exemplified in Fig. 4.

2. $p^2 < 0$. In this case, the lower curve in Fig. 3 corresponds to the profile of the refractive index. When deriving the reflectivity for the given $U(z)$ profile, one has to use the expression for the parameter t corresponding to formula (2.20):

$$\begin{aligned} t &= \tan \left(\sqrt{1 + x_2^2} \arctan u_2 \right), \\ u_2 &= \left(dL_2^{-1} \sqrt{1 - y^2} \right) (1 - ydL_2^{-1})^{-1}, \quad x_2 = \omega \Omega_2^{-1}. \end{aligned} \tag{4.16}$$

For an anomalous dispersion ($p^2 < 0$), the cutoff effect does not occur, and the characteristic frequency Ω_2 is defined by

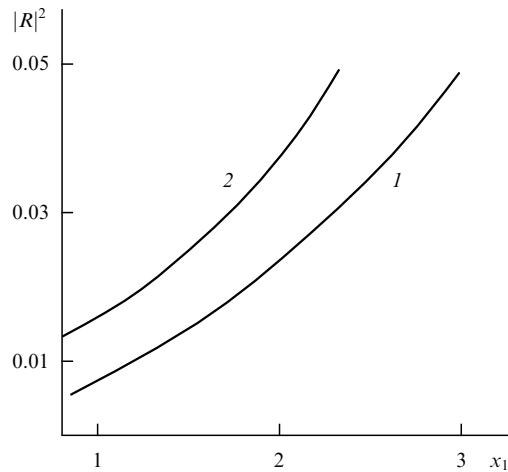


Figure 4. Broadband weakly reflecting domain in the power reflection spectrum $|R|^2$ of a nonuniform dielectric layer with a normal nonlocal dispersion (Fig. 3, curve 1). The normalized frequency x_1 is defined by expressions (4.15), $n_0 = 1.73$. The effect of layer thickness d and of the parameters L_1 and L_2 (2.11) is represented by curves 1 ($dL_2^{-1} = 0.15$) and 2 ($dL_2^{-1} = 0.3$); $y = 1$ in both cases.

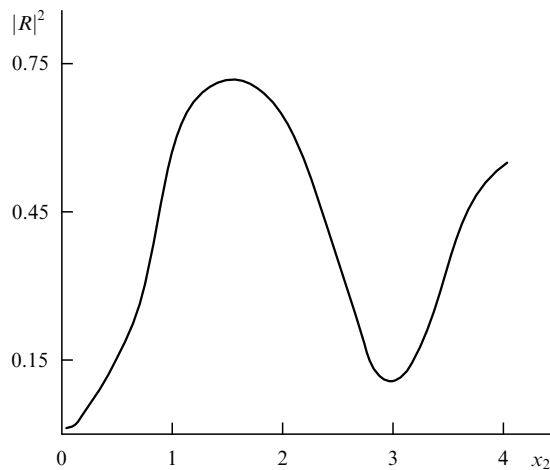


Figure 5. Spectral modulation of the reflection properties of a nonuniform dielectric layer of thickness d with an anomalous nonlocal dispersion (Fig. 3, curve 2). $|R|^2$ is the power reflectivity, x_2 is the normalized wave frequency (4.16); the profile of U is defined by expression (2.11), $L_2 = 1.5L_1$, $d = L_2$.

expressions (2.18). The frequency dependence of the reflectivity for this model is exemplified in Fig. 5.

We can now revert to the more general case of reflection from a nonuniform layer residing on the surface of an absorbing dielectric with a complex refractive index $n_2 + i\kappa_2$ (see Fig. 3). The reflection of a wave incident on the surface of an absorbing dielectric from vacuum is, as is well known, characterized by an absorption-dependent phase shift φ_κ [23]:

$$\tan \varphi_\kappa = 2\kappa(1 - n^2 - \kappa^2)^{-1}. \quad (4.17)$$

However, the reflection from a nonuniform transparent layer also gives rise to a phase shift controlled, in contrast to expression (4.17), by the profile of the refractive index. The mutual compensation of these shifts can substantially change the reflection properties of the system, resulting, in particular, in a weak reflection over a broad spectral range (Fig. 6).

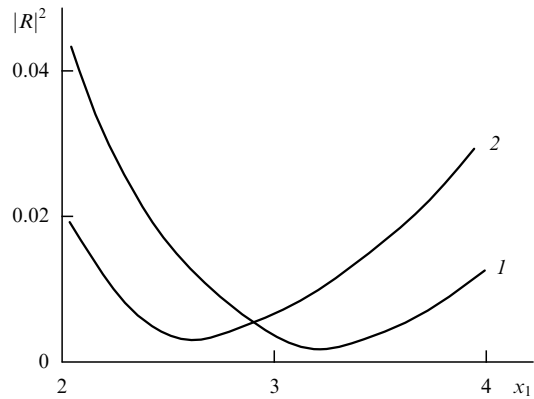


Figure 6. Suppression of the reflection properties of a dielectric with losses, coated with a nonuniform dielectric layer $U(z)$ (2.11). The suppression arises from the mutual compensation of the phase shifts, due to the losses and the nonuniformity, in the reflected wave. $|R|^2$ is the power reflectivity, x_2 is the normalized wave frequency; the effect of layer thickness d and parameters L_1 and L_2 is demonstrated by the curves 1 ($d = 0.25L_2$) and 2 ($d = 0.3L_2$). In both cases, $y = 0.25$.

As the characteristic nonuniformity lengths increase, the frequencies Ω_1 and Ω_2 tend to zero, while formulas (4.11)–(4.14) pass into the well-known result for the reflectivity of a uniform plate; in particular, for $\kappa_2 = 0$ in the limit $L_1 \rightarrow \infty$, $L_2 \rightarrow \infty$ we obtain

$$N_1 = U_1 = 1, \quad G_0 = G_1 = 0, \quad q\eta_1 = \omega n_0 d c^{-1} = \gamma,$$

$$\operatorname{Re} B = \frac{n_0^2 n_2^2}{n_2^2 \sin^2 \gamma + n_0^2 \cos^2 \gamma}, \quad \operatorname{Im} B = \frac{n_0(n_2^2 - n_0^2) \sin \gamma \cos \gamma}{n_2^2 \sin^2 \gamma + n_0^2 \cos^2 \gamma}. \quad (4.18)$$

The following tendencies characteristic of the reflection properties of nonuniform layers can be traced in Figs 4–6.

1. The cutoff frequency Ω_1 for a material with a given value of the refractive index n_0 depends on the characteristic lengths L_1 and L_2 . By varying the parameters L_1 and L_2 , it is possible to produce the cutoff effect in any spectral region. For instance, for $n_0 = 1.73$, $L_1 = 100$ nm, and $L_2 = 200$ nm, the Ω_1 frequency is equal to 1.25×10^{14} Hz. Referring to Fig. 4 (the curve corresponding to the value $\alpha = dL_2^{-1} = 0.15$), the power reflectivity $|R|^2$ of this layer for a thickness $d = 30$ nm is no higher than 5% over the spectral range $0.5 < \lambda < 1.5$ μm . The same curve shows that a nonuniform layer whose geometrical parameters are, say, ten times larger ($L_1 = 1000$ nm, $L_2 = 2000$ nm, $d = 300$ nm) provides a weak reflection ($|R|^2 < 0.05$) over a broad far-IR frequency range ($5 < \lambda < 15$ μm).

Therefore, by selecting the proper values of the parameters L_1 , L_2 , s_1 , and s_2 , it is possible to optimize the parameters of broadband reflectionless coatings for different spectral regions using Fig. 4. Figure 4, as well as Fig. 5 which follows, is plotted for normalized frequencies $x = \omega\Omega^{-1}$ and different thicknesses of the reflecting nonuniform layer. A more specific example of the effect of the $U(z)$ profile on the reflection spectrum of a layer with a given thickness appears in Fig. 7.

2. In the case of a nonuniform layer with an anomalous artificial dispersion ($p^2 < 0$), transmission and enhanced-reflection frequency bands (see Fig. 5) can form. For instance, the power reflectivity of a layer with the parameters

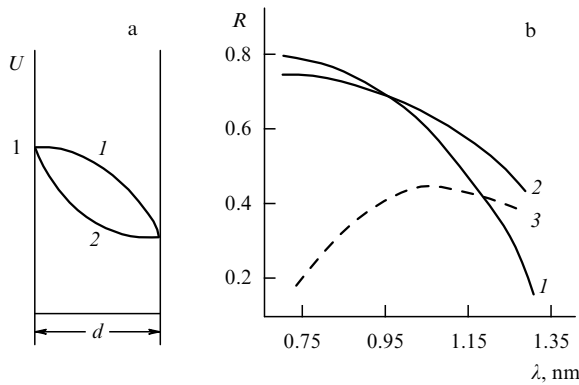


Figure 7. Effects of the gradient and the curvature of the $U(z)$ profile on the reflection spectrum of a nonuniform dielectric layer with a given thickness d : (a) $U(z)$ profiles (2.11) for the cases $s_1 = 0, s_2 = +1$ (curve 1) and $s_1 = +1, s_2 = -1$ (curve 2); (b) dependence of the power reflectivity on the wavelength λ . Curves 1 and 2 correspond to the reflection from the layers with the nonuniformity profiles 1 and 2 in Fig. 7a, $n_0 = 1.73, d = 120$ nm. Curve 3 is the reflection spectrum of a uniform layer with the same values of the refractive index n_0 and the thickness d .

$n_0 = 1.73, y = 0.75, L_2 = d = 900$ nm ($x_2 = 1.45$) for CO₂-laser radiation with a wavelength $\lambda = 10.2$ μm is $|R|^2 = 0.73$, as can be seen from Fig. 5. The value of this coefficient for the second harmonic radiation ($x_2 = 2.9$) is an order of magnitude lower: $|R|^2 = 0.07$. This property is of interest for the spectral filtration of separate field harmonics.

3. For a specific wavelength, the thickness of a nonuniform reflectionless layer can be several times smaller than the thickness of a uniform quarter-wave plate d_1 (4.1). In particular, for the wavelength $\lambda = 10.2$ μm and the refractive index $n_0 = 1.73$, the layer thickness d_1 is 1.45 μm ; at the same time, as seen from Fig. 4, the thickness of the nonuniform layer that limits the $\lambda = 10.2$ μm wave reflectivity to the level $R = 0.01$ ($\alpha = 0.15$) only 0.3 μm . This distinction can be used to optimize the parameters of reflectionless coatings.

Here, the reflection by a nonuniform dielectric is analyzed assuming the permittivity profile to be prescribed by expression (2.11). The profiles of the form (2.29) and (2.33) can be treated in a similar way. In particular, for profile (2.29), the wave field components can be obtained on substitution of expression (2.26) into expressions (2.19):

$$E_x = \frac{iA_2q}{\sqrt{U(z)}} \left[1 \mp \frac{i}{qL} \sqrt{1 - U(1 - M^2)} \right] \exp[i(q\eta - \omega t)], \quad (4.19)$$

$$H_y = iA_2n_0^2c^{-1}\omega\sqrt{U(z)} \exp[i(q\eta - \omega t)]. \quad (4.20)$$

The plus and minus signs in expression (4.19) correspond to the ascending and descending branches of the $U(z)$ profile (see Fig. 2); the phase path η is given by expression (2.35). By using the continuity conditions for the field components at the layer boundaries, it is possible to find the amplitude of the reflected wave within the K layer [see expression (4.9)] and calculate the reflectivity R . It is instructive to compare our approach to the calculation of the reflectivity of a nonuniform layer with the commonly used technique that involves the replacement of the smooth $U(z)$ distribution with a step-wise profile and the description of each layer with the use of Abeles

matrices [25]. On the one hand, the formalism of these matrices allows the reflectivity R of any multilayer coating to be determined numerically. On the other hand, a regular procedure for analyzing the reflectivity of these profiles — monotonic or nonmonotonic, symmetric or asymmetric — was constructed here with the aid of a set of $U(z)$ profiles involving several free parameters. Unlike a numerical calculation, the analytical solutions obtained allow several physical characteristics of nonuniform media to be revealed: the nonlocal dispersion, the cutoff frequency, and the transmission band. Moreover, unlike several exactly solvable models which result in complex hypergeometric functions [4], the structure of the field in the models considered in our work is expressed in terms of elementary functions, which facilitates and quickens the calculations.

5. Effects of the gradient and the curvature of the $\varepsilon(z)$ profile on the nonlocal dispersion of periodic nonsinusoidal dielectric structures

The wave reflection at the boundary of two uniform media, caused by the jumps of refractive index, is described by the well-known Fresnel formulas. The analysis of the reflection properties of a nonuniform layer performed in Section 4 reveals the dependence of wave reflection on the jump of the derivative of the refractive index [the G_0 factor in relationship (4.8)] at the layer boundary. The wave number q (2.10) in the model (2.11) is also dependent on the magnitude of L_1 . However, the model (2.11) also allows a more complicated effect to be revealed — the dependence of reflectivity on the second derivative of the refractive index of the medium, characterized by the parameter L_2 . It is this effect that may come to be the determining one in the wave reflection from a dielectric with a periodic nonuniformity $\varepsilon(z)$.

To demonstrate the contribution of the second derivative $\partial^2 U/\partial z^2$ to the efficiency of reflection, we consider the special case where the values of both the refractive index and its first derivative are continuous at the media interface. The geometry of the problem is shown in Fig. 8: a nonuniform layer of thickness d separates the domains with refractive indices n_1 ($z \leq 0$) and n_2 ($z \geq d$). The profile of the refractive index in the intervening layer $0 \leq z \leq d$ is composed of curves

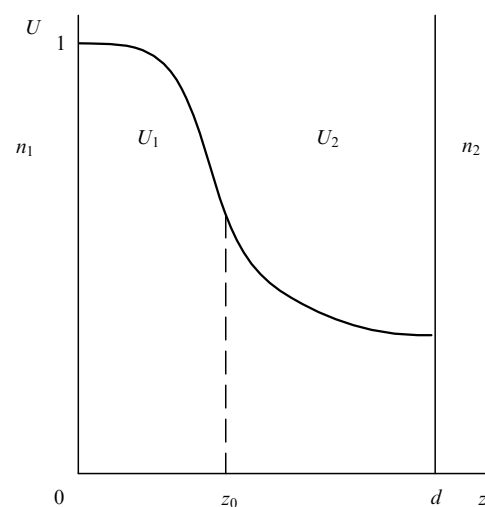


Figure 8. Smooth transition layer of thickness d composed of the curves U_1 and U_2 (5.1) which are tangent to one another at the point z_0 .

U_1 and U_2 :

$$U_1 = \left(1 + \frac{z^2}{L_2^2}\right)^{-1}, \quad U_2 = U_0 \left[1 + \frac{(d-z)^2}{l_2^2}\right]^{-1}, \quad U_0 = \frac{n_2}{n_1}. \quad (5.1)$$

The curves U_1 and U_2 are smoothly tangent to one another at some point z_0 . The values of the refractive index n are continuous at the layer boundaries $z = 0$ and $z = d$, the values of $\text{grad } n$ at the layer boundaries are equal to zero; however, the curvatures of the arcs U_1 and U_2 at the points $z = 0$ and $z = d$ are different:

$$\tilde{\kappa} = \frac{\partial^2 U / \partial z^2}{[1 + (\partial U / \partial z)^2]^{3/2}}, \quad \tilde{\kappa}_1 = -\frac{2}{L_2^2}, \quad \tilde{\kappa}_2 = \frac{2U_0}{l_2^2}. \quad (5.2)$$

At the point of tangency of the profiles U_1 and U_2 , the following conditions are fulfilled:

$$U_1 \Big|_{z=z_0} = U_2 \Big|_{z=z_0}, \quad \frac{\partial U_1}{\partial z} \Big|_{z=z_0} = \frac{\partial U_2}{\partial z} \Big|_{z=z_0}. \quad (5.3)$$

By substituting expressions (5.1) into conditions (5.3), it is possible to find the coordinate of the point of tangency and the relation between the parameters L_2 and l_2 which ensures the smoothness of tangency. We assume for definiteness that $n_2 < n_1$ and $U_0 < 1$ to obtain

$$z_0 = \frac{d}{\Delta_0}, \quad \frac{L_2^2}{d^2} \Delta_0 = \frac{U_0}{1 - U_0}, \quad \Delta_0 = 1 + \frac{U_0 l_2^2}{L_2^2}. \quad (5.4)$$

One of the parameters L_2 and l_2 in formulas (5.4) is free.

We consider a linearly polarized wave with a frequency ω incident normally from the $z < 0$ domain onto the boundary $z = 0$. For each of the media shown in Fig. 8, the vector potential of the wave field ψ (2.11) can be represented as

$$\begin{aligned} \psi &= \exp(ik_1 z) + R \exp(-ik_1 z), \quad z \leq 0, \\ \psi &= A_1 U_1^{-1/2} [\exp(iq_1 \eta_1) + Q_1 \exp(-iq_1 \eta_1)], \quad 0 \leq z \leq z_0, \\ \psi &= A_2 U_2^{-1/2} [\exp(iq_2 \eta_2) + Q_2 \exp(-iq_2 \eta_2)], \quad z_0 \leq z \leq d, \\ \psi &= D \exp(ik_2 z), \quad z \geq d. \end{aligned} \quad (5.5)$$

Here, R and D are the reflectivity and the transmittance of the nonuniform layer; the coefficients A_1 , A_2 , Q_1 , and Q_2 are determined from the conditions of continuity at the planes $z = 0$, $z = z_0$, and $z = d$. The wave numbers k_1 , k_2 , q_1 , q_2 and the quantities η_1 , η_2 are given by

$$k_{1,2} = \omega c^{-1} n_{1,2}, \quad q_{1,2} = k_{1,2} N_{1,2}, \quad N_1 = \sqrt{1 + \frac{c^2}{n_1^2 \omega^2 L_2^2}}, \quad N_2 = \sqrt{1 - \frac{c^2}{n_2^2 \omega^2 l_2^2}}, \quad (5.6)$$

$$\eta_1(z) = \int_0^z U_1 dz_1; \quad \eta_2(z) = \eta_1(z_0) + \int_{z_0}^z U_2 dz_1. \quad (5.7)$$

As seen from expressions (5.6), the wave numbers k_1 , k_2 , q_1 , and q_2 , which characterize the field structure in the four regions shown in Fig. 8, are different; thus, the reflected and transmitted waves are formed by reflections at the boundaries $z = 0$, $z = z_0$, and $z = d$. It is significant that the refractive index and its gradient are continuous at each of these planes

and the reflections originate at the points of inflection of the profile (5.2) owing to the jumps of the curvature $\tilde{\kappa}$ of the profile at these points. The calculation of the reflectivity is similar to that performed for a monotonic layer in Section 4. It is noteworthy that the quantities R and D are found employing the transformation (2.6) without expanding the periodic function into a Fourier series.

By combining the models (2.11) and (2.29), it is possible to construct more complex, deeply modulated, nonsinusoidal, periodic $U(z)$ profiles with a continuous distribution of the refractive index. In particular, of interest is a profile composed of convex (U_1) and concave (U_2) curves (2.11); in this case, the parameter values $s_1 = -1$, $s_2 = +1$ and $s_1 = +1$, $s_2 = -1$ correspond to the U_1 and U_2 functions. We assume for simplicity of analysis that these curves are tangent to one another at points z_n ($n = 1, 2, 3, \dots$) which lie in the straight line $U_1 = U_2 = 1$. For each arc U_n and U_{n+1} , the distance between the neighboring points of tangency $d_n = z_{n+1} - z_n$ and the slope of the tangents at these points are determined by the nonuniformity scale lengths L_1 and L_2 :

$$d_n = \frac{L_2^2}{L_1}, \quad \frac{\partial U}{\partial z} \Big|_{U=1} = \pm \frac{1}{L_1}. \quad (5.8)$$

The plus (minus) sign in expressions (5.8) corresponds to the passage from a convex (concave) arc to a concave (convex) one. The smoothness of tangency requires that the value of L_1 should be constant for all the arcs. Continuing the U profile with obedience to the condition $L_1 = \text{const}$ gives a smooth periodic distribution of the normalized profile of the refractive index of U shown in Fig. 9.

The resultant $U(z)$ distribution differs essentially from the frequently considered periodic structures arising from the harmonic modulation of the refractive index, specifically:

(1) the deviations of the maximum and the minimum of the $U(z)$ profile from the value $U = 1$ are not equal:

$$U_{\max} = (1 - y^2)^{-1}, \quad U_{\min} = (1 + y^2)^{-1}, \quad y = \frac{L_2}{2L_1}; \quad (5.9)$$

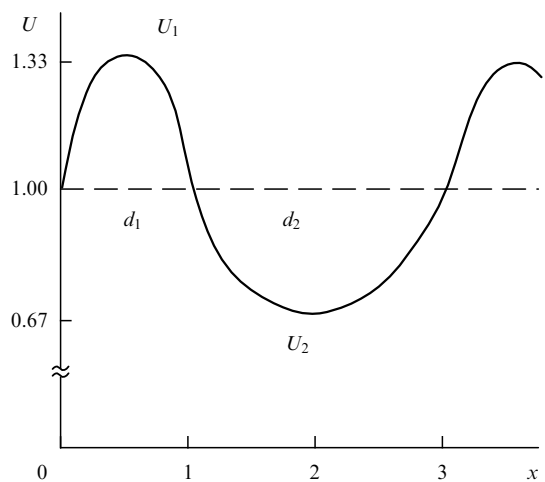


Figure 9. Spatial modulation of the profile of the normalized refractive index $U(x)$ composed of ‘modulation half-waves’ U_1 and U_2 (2.11), $x = zL_1^{-1}$; the ‘half-wave’ lengths d_1 and d_2 (5.8) correspond to the values $y_1^2 = 0.25$ and $y_2^2 = 0.5$.

(2) the ‘modulation half-wave’ lengths d_1 and d_2 (5.8) are different if the values of the parameter L_2 for the neighboring curves U_1 and U_2 are not equal;

(3) by composing a continuous profile W of curves (2.11) with different but periodically repetitive values of the L_2 parameter ($L_1 = \text{const}$), it is possible to find the reflectivities and the transmittances of modulated structures of complex symmetry, for instance, doubly periodic structures.

A periodic profile composed of the arcs U_1 and U_2 (see Fig. 2) is calculated in a similar manner. We compare expressions (2.28) and (2.32), which determine the slope of these curves, to obtain the condition for the smoothness of tangency of U_1 and U_2 at the points z_n which lie in the line $U_1 = U_2 = 1$:

$$\frac{M}{L} = \frac{M_1}{L_1}. \quad (5.10)$$

The wave numbers q_1 and q_2 (5.6) of the wave propagating through the portions U_1 and U_2 are different because $p^2 > 0$ and $p_1^2 < 0$, according to expressions (2.24) and (2.25). The wave propagation is therefore accompanied by reflections at the points z_n . Similar reflections also originate at the points of tangency of the arcs U_1 and U_2 (see Fig. 8), since the p^2 parameter values are not equal for the portions U_1 and U_2 :

$$p_1^2 = \frac{1}{4L_1^2} - \frac{1}{L_2^2}; \quad p_2^2 = \frac{1}{4L_1^2} + \frac{1}{L_2^2}. \quad (5.11)$$

Contrary to the cases considered above, a combination of the models (2.11) and (2.34) allows us to construct an interesting example of a continuous periodic $U(z)$ profile characterized by a constant value of the wave number q in the convex and concave portions of the profile. To this end, we represent the convex portion U_1 with the aid of expression (2.11), where $s_1 = +1$ and $s_2 = -1$, and the concave one, U_2 , with the aid of expression (2.29) and write down the condition for the equality of the wave numbers q_1 and q_2 :

$$\frac{1}{4L_1^2} + \frac{1}{L_2^2} = \frac{1}{L^2}. \quad (5.12)$$

The condition (5.12) should be fulfilled simultaneously with the condition for the profile smoothness at the points $U = 1$:

$$LL_1^{-1} = 2M. \quad (5.13)$$

We substitute expression (5.12) into condition (5.13) to obtain a relation between the parameters $y = L_2(2L_1)^{-1}$ and M for the modulation half-waves U_1 and U_2 at a smooth tangency:

$$y^2 = M^2(1 - M^2)^{-1}. \quad (5.14)$$

The profile (5.14) is shown in Fig. 10. However, even in this case ($q_1 = q_2$) the wave reflection is bound to occur at the point of tangency of the curves U_1 and U_2 . To make sure that this is the case, it would suffice to compare the expression for the field components in the U_1 domain, (4.2) and (4.3), with the corresponding field components in the U_2 domain, (4.19) and (4.20). For instance, the requirement for the electric field component that it be continuous for $z = d$, $U = 1$ would, in the absence of reflection, lead to the unsatisfiable condition $n_0 N(1 - iM) = 1$, where n_0 , N , and M are real quantities. The origination of reflection is associated with the jumps of the profile curvature at the point $z = d$.

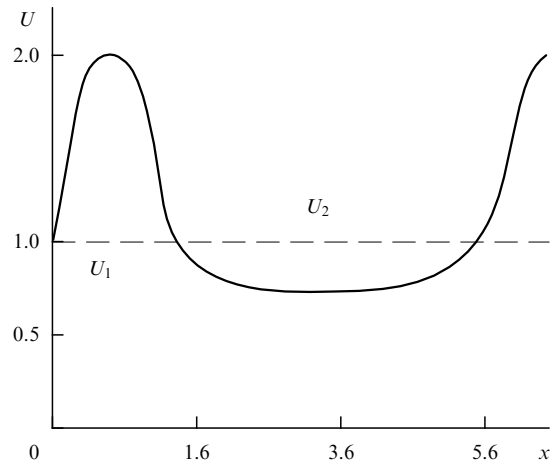


Figure 10. Modulated $U(x)$ profile, $x = zL^{-1}$, which provides a constant wave dispersion, as composed of curves U_1 (2.29) and U_2 (2.11), which are tangent at the level $U = 1$ (5.14). The wave numbers q in the domains U_1 and U_2 are determined by formulas (2.10) and (2.27), respectively; $M = 0.5$.

Therefore, the combination of the models (2.11)–(2.29) allows constructing broad classes of exactly solvable models of nonuniform dielectrics with nonsinusoidal periodic $\varepsilon(z)$ distributions. Within the framework of these models, it is possible to analytically represent the contribution of the jumps of the refractive index as well as of its first and second derivatives to the formation of reflected and transmitted waves.

6. Dispersion of high-frequency waves in plasmas with monotonic and nonmonotonic density distributions

The above consideration of the wave propagation through dielectric media implied the remoteness of resonance frequencies; it was assumed in this case that the local effects of material dispersion were negligible in comparison with the dispersion effects caused by the nonuniform permittivity distribution $\varepsilon(z)$. For a number of dielectrics, however, the $\varepsilon(z)$ nonuniformity may significantly alter the reflection and transmission wave spectra in the proximity of local resonances. These changes can be illustrated by the simple example of the propagation of high-frequency transverse waves in the electron plasma of a semiconductor with a nonuniform carrier density $N(z)$.

In studies of the wave processes in a nonuniform plasma, reference $N(z)$ distributions are of frequent use, which allow exact analytical solutions of the wave equation. In particular, for a linear density profile (1.5), the field structure in the plasma is, as is well known, represented in terms of the Airy functions [5]. For a parabolic profile, the exact solutions of the wave equation are given by the functions of parabolic cylinder [6]. However, the validity of these models, which contain only one free parameter L , is limited to plasma layers of finite thickness.

A more flexible model is treated below, which describes the ionization profile throughout the $z \geq 0$ half-space employing two parameters a and b [18],

$$W = \frac{N(z)}{N_0} = 1 - \frac{1}{b} + \frac{U^2(za^{-1})}{b}. \quad (6.1)$$

Here, the characteristic length a and the dimensionless quantity b are the free parameters of the model and N_0 is the ionization density at the medium boundary $z = 0$; the function $U(z a^{-1})$ satisfies the conditions

$$U \Big|_{z=0} = 1, \quad \lim_{z \rightarrow \infty} U = 0. \tag{6.2}$$

Therefore, the normalized electron density distribution (6.1) describes the ‘saturation’ of the ionization and the permittivity ε of the plasma with depth:

$$\lim_{z \rightarrow \infty} \varepsilon(z) = \varepsilon_L \left[1 - \frac{\Omega_0^2}{\omega^2} (1 - b^{-1}) \right],$$

$$\Omega_0^2 = \frac{4\pi e^2 N_0}{\varepsilon_L m_{\text{eff}}}. \tag{6.3}$$

Here, Ω_0 is the plasma frequency, m_{eff} is the effective carrier mass, and ε_L is the lattice contribution to the permittivity. The values of the parameter b in formula (6.1) lie in the ranges $b < 0$ and $b > 1$.

Now let us consider the propagation of an S -polarized wave in the medium (6.1) for $z \geq 0$. The direction of the y -axis is given by the k_{\parallel} component, which is perpendicular to the x -axis. The E_x , H_y , and H_z components of the wave field are interrelated by the Maxwell equations:

$$\frac{\partial E_x}{\partial z} = -\frac{1}{c} \frac{\partial H_y}{\partial t}, \quad \frac{\partial E_x}{\partial y} = \frac{1}{c} \frac{\partial H_z}{\partial t}, \tag{6.4}$$

$$\frac{\partial H_z}{\partial y} - \frac{\partial H_y}{\partial z} = \frac{\varepsilon_L}{c} \left[1 - \frac{\Omega_0^2}{\omega^2} (1 - b^{-1}) - \frac{\Omega_0^2 U^2(z)}{\omega^2 b} \right] E_x. \tag{6.5}$$

Expressing the field components in terms of the component $A_x = A_0 \psi$ of the vector potential (2.4), we transform the system (6.4), (6.5) into an equation for the function ψ :

$$\frac{\partial^2 \psi}{\partial z^2} + \frac{\partial^2 \psi}{\partial y^2} + \frac{\varepsilon_L \omega^2}{c^2} \left[1 - \frac{\Omega_0^2}{\omega^2} (1 - b^{-1}) - \frac{\Omega_0^2 U^2(z)}{\omega^2 b} \right] \psi = 0. \tag{6.6}$$

We rewrite Eqn (6.6) using the η -variable (2.6) and introducing a new function f :

$$\psi = f U^{-1/2} \exp[i(k_{\parallel} y - \omega t)]. \tag{6.7}$$

The function f satisfies the equation which follows from Eqn (6.6),

$$\frac{\partial^2 f}{\partial \eta^2} + f \left[\frac{p^2}{U^2} - \frac{\varepsilon_L \Omega_0^2}{c^2 b} - \frac{1}{2U} \frac{\partial^2 U}{\partial \eta^2} + \frac{1}{4U^2} \left(\frac{\partial U}{\partial \eta} \right)^2 \right] = 0, \tag{6.8}$$

$$p^2 = \frac{\varepsilon_L}{c^2} [\omega^2 - \Omega_0^2 (1 - b^{-1})] - k_{\parallel}^2. \tag{6.9}$$

To this point the function U , which determines the carrier density profile, has remained unknown. By using the η -variable, it is possible to construct models of both the monotonic and nonmonotonic ionization profiles $W(z)$ admitting exact analytical solutions of the wave equation (6.8).

1. A simple model of a monotonic ionization profile can be represented by the formula $U = \exp(-\eta a^{-1})$, where a is some characteristic length. However, this formula expresses the profile U as a function of the η -coordinate. To determine the

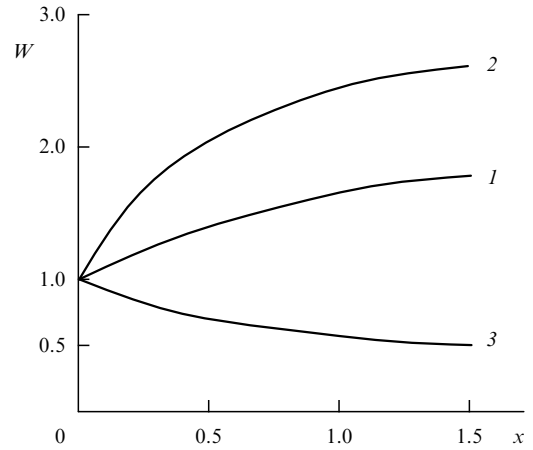


Figure 11. Plasma density profile $W(x)$, $x = zL^{-1}$ (6.1), which tends to the constant value $W = 1 - b^{-1}$ with depth in the plasma. The respective values of the b parameter for curves 1–3 are 2, -0.5 , and -1 . The function U in expression (6.1) is defined for curves 1 and 2 by expression (6.10) and for curve 3 by expression (7.11).

dependence of U in an explicit form, the expression $\eta = -a \ln U$ should be substituted into the definition of the η -variable. On solving the resultant equation, we find

$$U = \left(1 + \frac{z}{a} \right)^{-1}. \tag{6.10}$$

The $W(z)$ density profiles corresponding to the distribution (6.10) are shown in Fig. 11. We substitute expression (6.10) into Eqn (6.8) and go over to the new variable $u = U^{-1} = \exp(\eta a^{-1})$ to obtain the Bessel equation for the function f :

$$\frac{\partial^2 f}{\partial u^2} + \frac{1}{u} \frac{\partial f}{\partial u} + f \left(a^2 p^2 - \frac{q^2}{u^2} \right) = 0, \tag{6.11}$$

$$q^2 = \frac{\Omega_0^2 a^2 \varepsilon_L}{c^2 b} + \frac{1}{4}; \quad u = 1 + \frac{z}{a}. \tag{6.12}$$

The parameter p^2 was defined by expression (6.9).

We first consider the frequency range defined by the condition $p^2 > 0$. If $q^2 > 0$, the solution of Eqn (6.11) is represented by the Hankel function $H_q^{(1)}(apu)$. Reverting to the z -variable, we can represent the function ψ (6.7) as

$$\psi = \sqrt{1 + \frac{z}{a}} H_q^{(1)} [p(a + z)] \exp[i(k_{\parallel} y - \omega t)]. \tag{6.13}$$

We substitute the component $A_x = A_0 \psi$ of the vector potential into Eqns (2.4) to obtain the expressions for the components of the wave field:

$$E_x = i A_0 \omega c^{-1} \psi, \quad H_z = -i A_0 k_{\parallel} \psi,$$

$$H_y = \frac{A_0}{a} \left(\frac{1}{2u} + \frac{pa}{H_q^{(1)}(x)} \frac{\partial H_q^{(1)}(x)}{\partial x} \Big|_{x=pa u} \right) \psi. \tag{6.14}$$

By taking advantage of the asymptotic form of the Hankel functions

$$H_q^{(1)}(x) \Big|_{x \gg 1} = \sqrt{\frac{2}{\pi x}} \exp \left[i \left(x - \frac{\pi q}{2} - \frac{\pi}{4} \right) \right], \tag{6.15}$$

we can easily show that the components of the wave field deep in the medium ($z \gg a$), where the density nonuniformity vanishes, are represented by a traveling harmonic wave. For instance,

$$E_x \sim \exp[i(pz + k_{\parallel}y - \omega t)]. \quad (6.16)$$

The dispersion of a medium of this kind is described by Eqn (6.9).

The density nonuniformity in the proximity of the plasma boundary (6.1) can significantly alter the wave reflection spectrum. For simplicity we consider the case of normal wave incidence from the air onto the boundary of a solid-state plasma. We introduce the reflectivity R , which can be found from the conditions of continuity for the field components at the plane $z = 0$

$$\frac{1+R}{1-R} = \frac{2iac}{\omega} \left(1 + \frac{2ap}{H_q^{(1)}(x)} \frac{\partial H_q^{(1)}(x)}{\partial x} \Big|_{x=ap} \right)^{-1}. \quad (6.17)$$

By representing the Hankel function as the sum

$$H_q^{(1)} = I_q + iN_q,$$

where I_q and N_q are the Bessel and Neumann functions, and using the Wronskian of the pair of functions I_q and N_q

$$I_q(x) \frac{\partial N_q(x)}{\partial x} - N_q(x) \frac{\partial I_q(x)}{\partial x} = \frac{2}{\pi x}, \quad (6.18)$$

we obtain the complex reflectivity from expression (6.17):

$$R = \frac{-\operatorname{Re} Q + i(2\omega ac^{-1} - \operatorname{Im} Q)}{\operatorname{Re} Q + i(2\omega ac^{-1} + \operatorname{Im} Q)}, \quad (6.19)$$

$$\operatorname{Re} Q = -1 + \frac{2pa}{I_q^2 + N_q^2} \left(I_q \frac{\partial I_q}{\partial x} + N_q \frac{\partial N_q}{\partial x} \right),$$

$$\operatorname{Im} Q = \frac{4}{\pi} \frac{1}{I_q^2 + N_q^2}. \quad (6.20)$$

The argument of the Bessel and Neumann functions in formulas (6.20) is the quantity pa .

In the calculations using the formulas (6.19) and (6.20), the order q of the Hankel functions can assume any real values if the plasma density deep in the medium is lower than at the boundary. Otherwise ($b < 0$), the values of the parameter b are bounded by the condition $q^2 \geq 0$ (6.12).

An example of the frequency dependence of the reflectivity of a nonuniform electron plasma of InSb is given in Fig. 12 for the simple case $q = 1$ (6.12). Comparing curves 1 and 2 in this figure shows that the transition layer can significantly suppress the reflection capacity of a semiconductor plasma over a broad frequency range.

2. Models with a nonmonotonic ionization profile W can be represented in terms of the function

$$U(\eta) = \frac{\cosh(\eta/a_0 - \operatorname{arsinh} M)}{\sqrt{1+M^2}}, \quad M \geq 0. \quad (6.21)$$

Here, a_0 is the characteristic nonuniformity scale length and M is a free dimensionless parameter. By resolving formula (6.21) for η and substituting it into expression (2.6), we find an

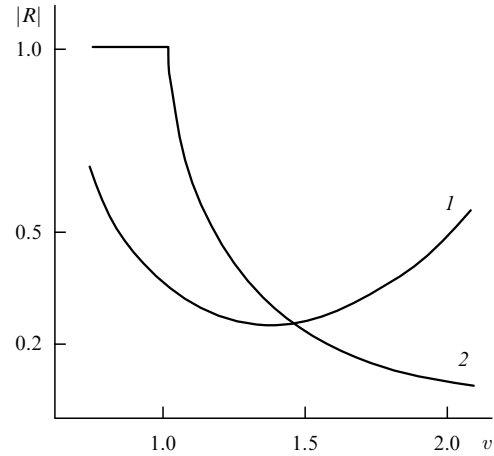


Figure 12. Modulus of the reflectivity R for a wave incident normally onto the surface of a nonuniform electron plasma of InSb ($\epsilon_L = 12.5$, $N_0 = 5 \times 10^{17} \text{ cm}^{-3}$) as a function of the normalized wave frequency $v = \omega\Omega_0^{-1}$ (curve 1). Profile of the carrier density is specified by Eqn (6.1); $b = 2$; the function U is given by expression (6.10), $a = 10^{-4} \text{ cm}$. Curve 2 is a plot of the reflectivity R for a uniform plasma ($a \rightarrow \infty$).

explicit expression for the $U(z)$ profile:

$$U(z) = \left(\cos \frac{z}{L} + M \sin \frac{z}{L} \right)^{-1}, \quad (6.22)$$

$$L = a_0 \sqrt{1+M^2}.$$

The distribution (6.22), defined in the interval $0 \leq z < z_\infty$, is minimum at the point z_m , where

$$\frac{z_m}{L} = \arctan M; \quad U_{\min} = \frac{1}{\sqrt{1+M^2}};$$

$$\frac{z_\infty}{L} = -\arctan \frac{1}{M}. \quad (6.23)$$

The function $U(z)$ (6.22) assumes the value $U = 1$ at the points 0 and z_1 :

$$\frac{z_1}{L} = \arcsin \frac{2M}{1+M^2}. \quad (6.24)$$

The points z_m (6.23) and z_1 lie in the domain of definition of the function $U(z)$: $z_m < z_1 < z_\infty$.

We substitute the $U(z)$ distribution (6.22) into expression (6.1) and consider the ionization profile, which comprises, in the interval $0 \leq z \leq z_1$, the convex arc (6.1), where $b_1 < 0$; the continuation of the profile in the interval is described by the concave arc (6.1) for $b_2 > 1$. The condition for the smoothness of tangency at the point z_1 relates the parameters of these profiles:

$$\frac{M_1}{M_2} = \frac{|b_1|L_1}{b_2L_2}. \quad (6.25)$$

By continuing to construct the sequence of such arcs, we will obtain a continuous, smooth, oscillatory ionization profile $N(z)$. The maxima and minima of this profile are

$$\frac{N_{\max}}{N_0} = 1 + \frac{1}{|b_1|} \frac{M_1^2}{1+M_1^2}; \quad \frac{N_{\min}}{N_0} = 1 - \frac{1}{b_2} \frac{M_2^2}{1+M_2^2}. \quad (6.26)$$

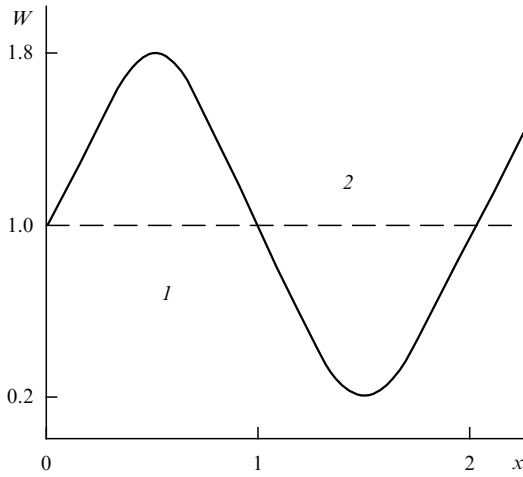


Figure 13. Deeply modulated harmonic plasma density distribution $W(x)$ described by formula (6.1), where the function U is defined by expressions (6.22). The parameter b in expression (6.1) for domains 1 and 2 is equal to ∓ 1 , $M = 2$, $x = zL^{-1}$. The modulation depth K is 80%.

In the simplest case, when $M_1 = M_2$ and $|b_1| = b_2$, a periodic electron density profile arises with the period $2z_1$ (6.24) shown in Fig. 13.

To find the wave field, for instance, in the domain $0 \leq z \leq z_1$, the function $U(\eta)$ (6.21) should be substituted into Eqn (6.8). We introduce a dimensionless variable x and rewrite Eqn (6.8) as

$$\frac{\partial^2 f}{\partial x^2} + f \left[q^2 - \frac{T}{\cosh^2 x} \right] = 0, \quad T = \frac{1}{4} - (pL_1)^2, \quad (6.27)$$

$$q^2 = \frac{1}{4} + \frac{\varepsilon_L \Omega_0^2 L_1^2}{c^2 |b_1|}, \quad x = \frac{\eta}{a_0} - \operatorname{arsinh} M. \quad (6.28)$$

An equation of the type (6.27) coincides formally with the Schrödinger equation of quantum mechanics which describes the particle scattering by the potential $\cosh^{-2} x$ [26]. In this case, there is good reason to emphasize once again that the potential $\cosh^{-2} x$ was defined here as a function of the ‘phase η -coordinate’; in the real space, the potential is defined by a different function (6.22). We go over to the new variable

$$u = \frac{1}{2}(1 - \tanh x)$$

and substitute the unknown function f of the form

$$f = (\cosh x)^{iq} F, \quad (6.29)$$

to obtain, for the function F , the hypergeometric equation

$$u(1-u) \frac{\partial^2 F}{\partial u^2} - [\gamma - u(1 + \alpha + \beta)] \frac{\partial F}{\partial u} - \alpha\beta F = 0, \quad (6.30)$$

$$\alpha, \beta = \frac{1}{2}(1 - 2iq \pm 2pL_1), \quad \gamma = 1 + iq.$$

Since the parameters α , β , and γ (6.30) are related as

$$\alpha + \beta + 1 = 2\gamma, \quad (6.31)$$

the fundamental solutions of Eqn (6.29) can be expressed in terms of the hypergeometric function G [27]:

$$F_1 = G(\alpha, \beta, \gamma, u), \quad F_2 = G(\alpha, \beta, \gamma, 1 - u). \quad (6.32)$$

By using expression (6.28) for the u -variable, it is possible to write the solution of the equation for the vector potential ψ (6.7) as

$$\psi = \sqrt{\cos \frac{z}{L} + M \sin \frac{z}{L}} (\cosh x)^{iq} \exp[i(k_{\parallel} y - \omega t)] \times [G(\alpha, \beta, \gamma, u_-) + SG(\alpha, \beta, \gamma, u_+)]. \quad (6.33)$$

Here, S is a constant determined from the boundary conditions and G is the hypergeometric function of the argument

$$u_{\mp} = \frac{1}{2}(1 \mp \tanh x). \quad (6.34)$$

The solutions of Eqn (6.7) in the adjacent domain $z_1 \leq z \leq z_2$, which corresponds to the concave arc of the W profile (see Fig. 13), can be constructed in a similar way (6.33). By invoking the conditions for the continuity of the field components at the points $z = 0, z_1, z_2, \dots$, it is possible to investigate the field structure in a plasma with a periodic profile of electric density. To calculate the field at these points, the corresponding values of the x -variable (6.28) should be found. These values can be obtained on substitution of the function $U(z)$ (6.22) into formula (2.6):

$$x = -\operatorname{arsinh} M + \ln \left| \frac{1 + m_+ \tan(z/2L)}{1 - m_- \tan(z/2L)} \right|, \quad (6.35)$$

$$m_{\pm} = \sqrt{1 + M^2} \pm M.$$

Upon substituting the values $z = 0$ and z_1 (6.24) into expression (6.35), we have

$$x \Big|_{z=0} = -\operatorname{arsinh} M, \quad x \Big|_{z=z_1} = \operatorname{arsinh} M. \quad (6.36)$$

For $z \rightarrow z_{\infty}$ (6.23), the x -variable (6.35) increases indefinitely. The resultant values of x (6.36) are used to calculate the values of the function f (6.33) at the points of inflection $z = 0, z_1, z_2, \dots$, etc., which separate the concave and convex portions of the W profile. The difference between these values determines the wave reflection at the points of inflection of the periodic ionization profile involved.

By combining the $U(z)$ distributions (6.10) and (6.22), it is possible to find the field structure in plasmas with nonmonotonic ionization profiles; this refers, for instance, to the density distribution (6.1) composed of the convex arc U (6.22), where $b = -b_1$ ($b_1 > 0$), and the monotonically decreasing function U (6.10), where $b = b_2 > 1$. The condition for the smoothness of tangency of these curves at the level $U = 1$ is of the form

$$\frac{M}{|b_1|L} = \frac{1}{b_2 a}. \quad (6.37)$$

The resultant nonmonotonic carrier density distribution, which is characterized by the single peak N_{\max} and which tends to the constant value N_c deep in the medium, is given in Fig. 14 (curve I):

$$\frac{N_{\max}}{N_0} = 1 + \frac{M^2}{|b_1|(1 + M^2)}, \quad \frac{N_c}{N_0} = 1 - \frac{Ma}{|b_1|L}. \quad (6.38)$$

This distribution contains four free parameters: M , b_1 , L , and a . A similar distribution of N , characterized, unlike the

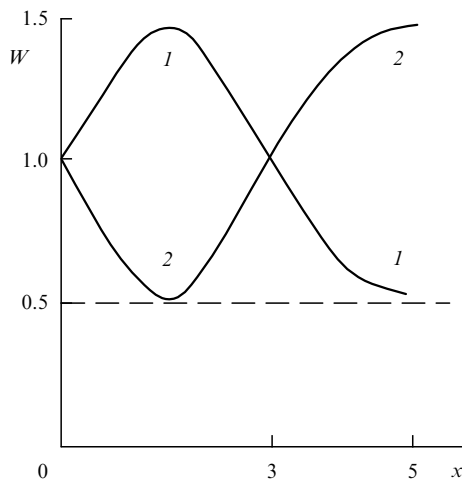


Figure 14. Nonmonotonic profiles of the normalized plasma density W (6.1), $x = zL^{-1}$. For curve 1, $b_1 = -1$ and $b_2 = 1$. For curve 2, $b_1 = 2$ and $b_2 = -2$. The function U is defined by expressions (6.22) and (6.10) in the ranges of the dimensionless coordinate $0 \leq x \leq \pi$ and $x \geq \pi$, respectively; $M = 1$.

distribution (6.38), by a single negative peak N_{\min} ,

$$\frac{N_{\min}}{N_0} = 1 - \frac{M^2}{b_1(1+M^2)}, \quad \frac{N_c}{N_0} = 1 + \frac{Ma}{b_1L}, \quad (6.39)$$

is shown in Fig. 14 (curve 2).

To calculate the reflectivities and the transmittances of a nonuniform plasma described by the curve (6.22), the hypergeometric functions $G(\alpha, \beta, \gamma, u)$ should be tabulated. One way to independently verifying the precision of this tabulation is to consider, in the context of Eqn (6.27), a simple problem of wave propagation, for the parameter T in Eqn (6.27) equal to zero, i.e., $4(pL_1)^2 = 1$. In this case, the solution of Eqn (6.27) is described by the harmonic wave

$$f = \exp(iqx) + S \exp(-iqx), \quad (6.40)$$

where the wave number q and the x -coordinate are defined by expressions (6.28) and (6.35). By using the solution (6.40), it is easy to find, for instance, the reflectivity of a nonuniform plasma layer containing one ‘half-wave’ of the spatially modulated carrier density (see Fig. 13). On the other hand, this reflection coefficient can be calculated in the context of the general approach with a recourse to the eigenfunctions ψ . Comparing the results would allow an estimation of the precision of the calculations with the use of hypergeometric functions.

As seen from Figs 11–14, the use of the phase coordinate considerably extends the scope of exactly solvable models in the problems of wave propagation in nonuniform dispersion media. The reflection properties of such media are significantly changed due to the coordinate dependence (see Fig. 12), which results in the formation of broad low-reflectivity spectral intervals. The resultant analytical solutions, which contain several free parameters, allow the wave reflection spectra to be studied over a broad parameter range. An alternative statement of the reflection problem involves a search for a medium nonuniformity profile which provides broadband reflectionless wave passage through the medium boundary. Examples of such profiles for normal wave

incidence onto the boundary of a dielectric described by the Debye or Lorentz models for constant values of the parameters Ω_0 and ε_L were found by numerical techniques in Ref. [28].

7. Surface electromagnetic waves in a nonuniform dielectric

In the foregoing, the propagation of electromagnetic fields along the direction of the gradient of $\varepsilon(z)$ in a nonuniform dielectric was discussed. However, the $\varepsilon(z)$ nonuniformity can significantly affect the dispersion properties of the waves which propagate in the direction perpendicular to $\nabla\varepsilon$, in particular, the waves on the surface of a nonuniform medium. Effects of this type, which are known in the radio and IR ranges [23], can be conveniently considered by the example of a surface wave in a nonuniform plasma medium.

For an abrupt boundary between two uniform media, characterized by a jump of the permittivity, the localization of waves in the vicinity of this boundary is possible only on condition that [29]

- (i) the spectrum of surface waves in the plasma has an upper bound $\omega_c = \Omega_0/\sqrt{2}$, where Ω_0 is the plasma frequency;
- (ii) all the components of the surface wave field decay exponentially with depth within the medium, the characteristic decay depth being the same for all the components;
- (iii) the polarization structure of the surface wave propagating in the y -direction close to the boundary $z = 0$ is determined by two electric components E_y and E_z and a single magnetic component H_x (the TM wave).

The interest in the properties of surface electromagnetic waves (SEWs) in a plasma with a blurred boundary fostered the development of a two-layer model. This model corresponds to a plasma layer with a finite thickness and a linear ionization profile, adjacent to a half-space bounded by a conventionally adopted plane and filled with a uniform plasma. The TM-polarized waves in this system, which resembles a strip line with a nonuniform cross section placed on a uniform substrate, were considered in Ref. [30].

In contrast, the surface waves in a nonuniform plasma are considered here within the framework of the method of the phase coordinate η (2.6). Employing this method does not necessitate invoking conventional boundaries in the bulk of the medium, which are inherent in the multilayer model, and furnishes the possibility of obtaining exact analytical solutions for the surface wave fields in a plasma with a continuous density distribution. This approach makes it possible to reveal branches of surface waves not subject to the limitations (i)–(iii), which are intrinsic in the waves at the surface of the media with an abrupt interface.

Some of the results of Section 6 can be used in the analysis of the problem under consideration. We begin with the Maxwell equations for an S -polarized wave with the components E_x , H_y , and H_z (6.4), (6.5), which propagates through the plasma with a carrier density profile prescribed by expression (6.1). Assuming that the carrier density distribution is defined by the function $U = (1 + za^{-1})^{-1}$ (6.10), we arrive at Eqns (6.11) and (6.12) for the vector potential of the wave field. The solutions of the resultant Eqn (6.11) depend on the values of the parameter p^2 . The domain $p^2 > 0$ considered in Section 6 corresponds to the waves which travel deep inside the nonuniform plasma. The solutions of Eqn (6.11) for negative values of the parameter p^2 (6.9) are constructed below.

The solutions of Eqn (6.11) for $p^2 < 0$ are the modified Bessel functions $K_q(z)$, whose values decrease with the increase of the z -coordinate. These functions describe the structure of the field localized near the plasma boundary $z = 0$. By introducing the designation $p_1^2 = -p^2 > 0$, it is possible to represent the function ψ (6.7) as

$$\psi_1 = \sqrt{1 + \frac{z}{a}} K_q[p_1(a+z)] \exp[i(k_s y - \omega t)]. \quad (7.1)$$

The wave field components in the medium ($z \geq 0$) can be found by substituting expression (7.1) into Eqns (2.4):

$$\begin{aligned} E_x &= iA_1 \omega c^{-1} \psi_1 = e_x E_x \Big|_{z=0}, \\ H_z &= iA_1 k_s \psi_1 = h_z H_z \Big|_{z=0}, \\ H_y &= -\frac{A_1}{a} \left[\frac{1}{2u} + \frac{1}{K_q(pu)} \frac{\partial K_q(pu)}{\partial u} \right] \psi_1, \\ u &= 1 + za^{-1}. \end{aligned} \quad (7.2)$$

To calculate the components of the field localized in the air close to the plasma boundary, we first find the corresponding function ψ_0 from Eqn (6.6) by putting $\Omega_0 = 0$ and $\varepsilon_L = 1$:

$$\psi_0 = \exp \left[i(k_s y - \omega t) + \frac{z}{l} \right]. \quad (7.3)$$

Here, l is the characteristic scale length for the decay of the surface wave in the air. We substitute expression (7.3) into Eqns (2.4) to determine the values of E_x , H_y , and H_z in the air:

$$E_x = iA_0 \omega c^{-1} \psi_0, \quad H_y = -A_0 l^{-1} \psi_0, \quad H_z = iA_0 k_s \psi_0. \quad (7.4)$$

The dispersion equation which relates ω , k_s , and l follows from the Maxwell equations (6.4) and (6.5):

$$k_s^2 = \frac{\omega^2}{c^2} + \frac{1}{l^2}. \quad (7.5)$$

By comparing the field components in the air (7.4) and in the plasma (7.2) and invoking the conditions of continuity at the boundary $z = 0$ ($u = 1$), we obtain the relationships

$$\frac{a}{l} = \frac{1}{2} + \frac{1}{K_q(pa)} \frac{\partial K_q(pau)}{\partial u} \Big|_{u=1}. \quad (7.6)$$

Note that the left-hand side of equality (7.6) is positive and the derivative of the decaying K_q function is negative. Since the limiting value of the second term in relationships (7.6) is equal to $-q$, the constraint $al^{-1} > 0$ limits the values of the q index in the expression for the vector potential ψ_1 (7.1):

$$\frac{1}{2} \geq q \geq 0. \quad (7.7)$$

As seen from the definition of the q index (6.12), condition (7.7) can be fulfilled only for negative values of the parameter b of the carrier density distribution (6.1). These values correspond to the growth of the carrier density deep in the plasma (see Fig. 11).

The spectra of surface waves in a nonuniform plasma obtained by solving Eqns (7.5) and (7.6) in combination are given in Fig. 15. These spectra essentially depend on the parameters a and b in the carrier density distribution (6.1). The field decay scale length in the air, l , determined from Eqn (7.5), also depends on these parameters. As is clear from the condition for the existence of SEWs ($p^2 < 0$), their frequencies are bounded from above:

$$\omega^2 \leq \omega_c^2 = \Omega_0^2 (1 + |b|^{-1}) + k_s^2 c^2 \varepsilon_L^{-1}. \quad (7.8)$$

In the domain of low values of the parameter pa ($pa \ll 1$), it is possible to obtain an approximate dispersion equation for the waves under study even without a numerical solution of the system (7.5), (7.6):

$$k_s^2 = \frac{\omega^2}{c^2} + \frac{1}{a^2} \left(\frac{1}{2} - q \right)^2. \quad (7.9)$$

The surface waves whose spectra are shown in Fig. 15 propagate along the plane air–plasma interface. However, when a wave is obliquely incident from the air onto the plasma, the projection of the wave vector k_{\parallel} onto this plane is always smaller than the modulus of the wave vector of the plasma wave k_s (7.9). To excite a surface wave in this case, the magnitude of k_{\parallel} should be increased, for instance, by passing the incident wave through a prism with a refractive index $n > 1$ located on the $z = 0$ plane [29]. In this case, the condition for matching the incident and surface waves has the form

$$n \sin \gamma = k_s c \omega^{-1}. \quad (7.10)$$

Referring to Fig. 15, the condition for the excitation of a SEW (7.10) can be fulfilled over a broad IR frequency range.

The above analysis shows how the prerequisites to the existence of surface electromagnetic waves (i)–(iii) change if at least one of the contiguous media is nonuniform:

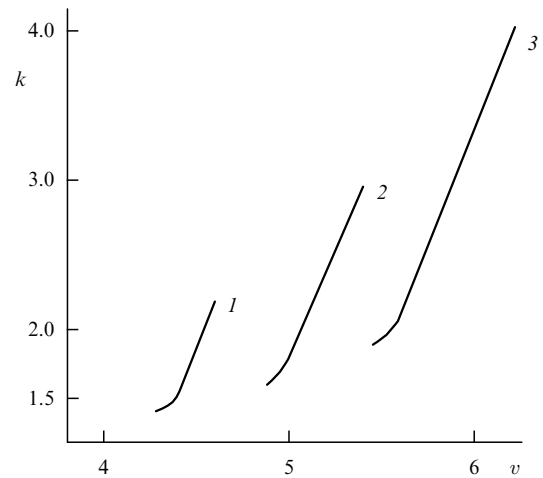


Figure 15. Spectra of TE-polarized surface waves in a nonuniform electron plasma of InSb ($\varepsilon_L = 12$, $N_0 = 3 \times 10^{16} \text{ cm}^{-3}$, $a = 10^{-4} \text{ cm}$, $m_{\text{eff}} = 0.01m_0$), $k_s = k \times 10^3 \text{ cm}^{-1}$, $\omega = v \times 10^{13} \text{ rad s}^{-1}$. The normalized distribution of the carrier density is described by the models (6.1) and (6.10), $x = za^{-1}$. Curves 1–3 correspond to different values of W deep in the medium; the dimensionless parameter b for these curves is equal to -0.7 , -0.5 , and -0.4 , respectively.

(1) the spectrum of surface waves broadens: in lieu of the limitation $\omega < \Omega_0/\sqrt{2}$, the condition (7.8) arises, which is indicative of the existence of a SEW with a frequency higher than the plasma frequency Ω_0 at the surface $z = 0$;

(2) unlike the monotonic exponential decay of all the SEW components in a uniform medium, the spatial structure of surface waves in a nonuniform plasma (7.2) is nonmonotonic: the E_x and H_z components pass through a maximum while the H_y component is sign-variable (Fig. 16);

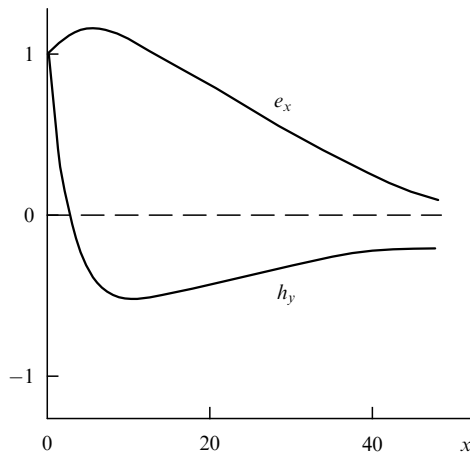


Figure 16. Spatial structure of the normalized field components of a TE-polarized surface wave deep within a nonuniform plasma (see Fig. 15, $b = -0.5$). Curves 1 and 2 correspond to the components e_x and h_y (7.2), $x = za^{-1}$.

(3) the electromagnetic wave at the surface of a nonuniform plasma is TE-polarized; it should be mentioned that a TE-polarized SEW at the boundary of a granular medium was reported in Ref. [31].

Eqn (6.8) can be used to analyze the SEW in a plasma for other carrier density profiles as well. Consider, for instance, the distribution (6.1) for an exponential variation of the function $U(z)$ (see Fig. 11, curve 3):

$$U = \exp\left(-\frac{z}{a}\right) = 1 - \eta a^{-1}. \tag{7.11}$$

We substitute expression (7.11) into Eqn (6.8) and introduce a new function Q to obtain

$$Q = \frac{f}{\sqrt{U}}; \quad \frac{\partial^2 Q}{\partial x^2} + \frac{1}{x} \frac{\partial Q}{\partial x} + Q \left(v^2 + \frac{p^2 a^2}{x^2} \right) = 0, \tag{7.12}$$

$$x = \exp\left(-\frac{z}{a}\right); \quad v^2 = \frac{\varepsilon_L \Omega_0^2 a^2}{|b|c^2}. \tag{7.13}$$

The solution of Eqn (7.12), which decays with depth in the medium and corresponds to the case $b < 0$, $p^2 = -g^2 \leq 0$, can be expressed in terms of the Bessel function $I_{ga}(vx)$. Reverting to the z -variable, we obtain an expression for the component of the vector potential of a surface wave ψ (6.7):

$$\psi = I_{ga} \left[v \exp\left(-\frac{z}{a}\right) \right] \exp[i(k_s y - \omega t)]. \tag{7.14}$$

We substitute the function ψ (7.14) into Eqns (2.4) to obtain the field components in the plasma. The asymptotic

form of the Bessel functions for small values of the argument x ,

$$I_n(x) \Big|_{x \ll 1} \approx \left(\frac{x}{2}\right)^n \frac{1}{\Gamma(n+1)}, \tag{7.15}$$

where Γ is the gamma-function, shows that the field components decay exponentially with depth in the medium:

$$I_{ga} \left[v \exp\left(-\frac{z}{a}\right) \right] \Big|_{z \gg a} = \left(\frac{v}{2}\right)^{ga} \frac{\exp(-gz)}{\Gamma(1+ga)}. \tag{7.16}$$

With the use of the continuity conditions for the field components in the air (7.4) and in the medium for $z = 0$, we obtain, in view of Eqn (7.5), a SEW dispersion equation of the form

$$\frac{v [I_{ga-1}(v) - I_{ga+1}(v)]}{2I_{ga}(v)} = \sqrt{(k_s a)^2 - \left(\frac{\omega a}{c}\right)^2}. \tag{7.17}$$

The domain of existence of such waves, which is defined by the condition $g^2 \geq 0$, coincides with that defined by condition (7.8). In the special case of $v \ll 1$, Eqn (7.17) can be simplified using the asymptotics (7.15):

$$(k_s a)^2 - \left(\frac{\omega a}{c}\right)^2 = \left[1 + ag - \frac{v^2}{4ag} \right]^2. \tag{7.18}$$

We should emphasize the difference between the SEW dispersion equations (7.6) and (7.17) and their respective approximations (7.9) and (7.18). These equations describe models of a nonuniform plasma wherein the carrier densities at the surface $U|_{z=0} = 1$ and at the depth $U|_{z \gg a} = 1 - b^{-1}$ coincide; moreover, the values of the density gradients near the surface $z = 0$ also coincide. The difference in the SEW spectra of these models, which are defined by Eqns (7.6) and (7.17), is related to the carrier density distribution W deep in the medium (see Fig. 11). This SEW field sensitivity to the profile of W may be of interest for the density diagnostics of a nonuniform plasma through the use of surface electromagnetic waves.

8. Dispersion properties of nonstationary dielectrics

Wave phenomena in media whose electromagnetic characteristics are time-dependent are the key to understanding a variety of problems of space physics [32], short-pulse wave dynamics in continuous media [33], and optical diagnostics of fast processes [34]. Temporal variations in permittivity can radically alter the reflection and refraction properties of such media. Unlike the Doppler effect, where the tuning of the reflected wave is related to the reflector motion, the subject to be discussed here is the time evolution of electromagnetic fields in immobile media whose permittivity is a function of time t .

An important characteristic of such nonstationary wave processes is a finite relaxation time of the electromagnetic parameters of the medium and, in particular, its permittivity. Individual cases that correspond to adiabatic periodic variations of $\varepsilon(t)$ and a linear variation of $\varepsilon(t)$ were considered in Refs [11, 35]. However, in a number of problems, both applied and academic, situations occur whereby the period of field oscillation T and the medium

relaxation time t_0 prove to be of the same order of magnitude. In these instances the ratios $t_0 T^{-1}$ or $T t_0^{-1}$ are not small parameters, and exact analytical solutions of the Maxwell equations with time-dependent coefficients are required to analyze the wave problems. Here, such solutions are constructed for simple models assuming that the dynamics of medium relaxation are determined by factors independent of the wave field, for instance, by heating, ionization, or phase transitions [36]. In particular, such a model is of interest for the analysis of fast relaxation processes in media perturbed by a laser pulse [37]. In the context of this model, the induction D of the field E in the medium can be represented as

$$D(t) = \varepsilon(t)E(t); \quad \varepsilon(t) = n_0^2 U^2(t). \tag{8.1}$$

Here, n_0 is the refractive index of the medium prior to the onset of the relaxation process and the dimensionless $U(t)$ function describes the dynamics of this process. For simplicity we neglect the wave absorption in what follows, i.e., the $\varepsilon(t)$ dependence is described by a real $U(t)$ function. Three problems should be solved to find the reflection and the refraction of electromagnetic waves at the medium boundary (8.1);

(i) to construct solutions of the Maxwell equations for the medium (8.1);

(ii) to find explicit expressions for the functions $U(t)$ which lead to such solutions;

(iii) to generalize the Fresnel formulas for the description of wave reflection by the media characterized by the functions $U(t)$.

These problems for nonstationary media can be conveniently considered developing the method of the phase coordinate, which was previously employed in the optics of nonuniform dielectrics (see Section 2). By analogy with the phase coordinate η (2.6), we introduce a τ -variable, which has the dimensionality of time:

$$\tau = \int_0^t \frac{dt_1}{U(t_1)}, \tag{8.2}$$

This permits us to find broad classes of analytical solutions for nonstationary Maxwell equations in the form of traveling waves. Such solutions make it possible to represent, in an explicit form, the effect of the finite relaxation time of the medium permittivity on the wave dispersion.

To demonstrate the principal stages of this approach, we consider a normal incidence of waves from vacuum onto the half-space $z \geq 0$ occupied with a nonstationary dielectric (8.1). In this half-space, the propagation of a linearly polarized wave with the components E_x and H_y in the z -direction is described by the Maxwell equations

$$\frac{\partial E_x}{\partial z} = -\frac{1}{c} \frac{\partial H_y}{\partial t}; \quad -\frac{\partial H_y}{\partial z} = \frac{1}{c} \frac{\partial D_x}{\partial t}. \tag{8.3}$$

Let us solve the problems (i)–(iii) for the system of equations (8.3).

Problem (i). By extending the analogy with the approach described in Section 2, it is possible to solve the system (8.3) in two ways.

1. By expressing the field components E_x and H_y in terms of the function ψ_1 (2.4), we reduce the first of Eqns (8.3) to an identity; in this case, the second equation in (8.3) assumes the form

$$\frac{\partial^2 \psi_1}{\partial z^2} - \frac{n_0^2 U^2(t)}{c^2} \frac{\partial^2 \psi_1}{\partial t^2} = \frac{n_0^2}{c^2} \frac{\partial U^2}{\partial t^2} \frac{\partial \psi_1}{\partial t}. \tag{8.4}$$

We introduce the new function

$$F_1 = \psi_1 \sqrt{U(t)} \tag{8.5}$$

and, using the τ -variable (8.2), rewrite Eqn (8.4):

$$\frac{\partial^2 F_1}{\partial z^2} - \frac{n_0^2}{c^2} \frac{\partial^2 F_1}{\partial \tau^2} = -\frac{n_0^2}{c^2} F_1 \left[\frac{U}{2} \frac{\partial^2 U}{\partial t^2} + \frac{1}{4} \left(\frac{\partial U}{\partial t} \right)^2 \right]. \tag{8.6}$$

Although the function $U(t)$ is still unknown, the transformations (8.2) and (8.4) allowed us to eliminate the time-dependent coefficient in the left-hand side of Eqn (8.4); the nonstationary effect is described by the expression bracketed in the right-hand side of Eqn (8.6).

To determine the dependence $U(t)$, we consider a simple case where the expression in the square brackets in Eqn (8.6) is equal to some constant $-p_1^2$:

$$\frac{U}{2} \frac{\partial^2 U}{\partial t^2} + \frac{1}{4} \left(\frac{\partial U}{\partial t} \right)^2 = -p_1^2. \tag{8.7}$$

In this case, all the coefficients of Eqn (8.6) are constant [37]:

$$\frac{\partial^2 F_1}{\partial z^2} - \frac{n_0^2}{c^2} \frac{\partial^2 F_1}{\partial \tau^2} = \frac{n_0^2 p_1^2}{c^2} F_1. \tag{8.8}$$

The solution of Eqn (8.8) can be written in the form of a traveling wave:

$$F_1 = \exp[i(q_1 z - \omega \tau)], \quad q_1 = \omega n_0 c^{-1} N, \quad N = \sqrt{1 - p_1^2 \omega^{-2}}. \tag{8.9}$$

We substitute expression (8.9) into the equality (8.5) to obtain an expression for the function ψ_1 :

$$\psi_1 = \frac{A_1 \exp[i(q_1 z - \omega \tau)]}{\sqrt{U(t)}}. \tag{8.10}$$

Here, A_1 is the normalizing constant. With the use of relations (2.4), we find expressions for the field components in the nonstationary medium:

$$E_x = \frac{i\omega}{cU(t)} \left(1 - \frac{i}{2\omega} \frac{\partial U}{\partial t} \right) \psi_1, \quad H_y = iq_1 \psi_1. \tag{8.11}$$

2. An alternative way of solving the system (8.3) involves representing the field components in terms of an auxiliary function ψ_2 by analogy with formulas (2.19):

$$E_x = \frac{1}{n_0^2 U^2(t)} \frac{\partial \psi_2}{\partial z}; \quad H_y = \frac{1}{c} \frac{\partial \psi_2}{\partial t}. \tag{8.12}$$

Unlike the first way of solution, on substitution of expressions (8.12) into the system (8.3), the second of Eqns (8.3) is identically fulfilled and the first one assumes the form

$$\frac{\partial^2 \psi_2}{\partial z^2} - \frac{n_0^2 U^2(t)}{c^2} \frac{\partial^2 \psi_2}{\partial t^2} = 0. \tag{8.13}$$

We introduce a new function $F_2 = \psi_2 U^{-1/2}$ and, using the τ -variable, rewrite Eqn (8.13) as

$$\frac{\partial^2 F_2}{\partial z^2} - \frac{n_0^2}{c^2} \frac{\partial^2 F_2}{\partial \tau^2} = \frac{n_0^2}{c^2} F_2 \left[\frac{U}{2} \frac{\partial^2 U}{\partial t^2} - \frac{1}{4} \left(\frac{\partial U}{\partial t} \right)^2 \right]. \tag{8.14}$$

By equating the expression bracketed in the right-hand side of Eqn (8.14) to some constant p_2^2 ,

$$\frac{U}{2} \frac{\partial^2 U}{\partial t^2} - \frac{1}{4} \left(\frac{\partial U}{\partial t} \right)^2 = p_2^2, \tag{8.15}$$

we arrive once again at an equation with constant coefficients, which coincides, after the change $p_2 \rightarrow p_1$, with Eqn (8.8). By writing down the solution of this equation in the form of a traveling wave, we can represent the function ψ_2 as

$$\psi_2 = A_2 \sqrt{U(t)} \exp[i(q_2 z - \omega \tau)], \tag{8.16}$$

$$q_2 = \omega n_0 c^{-1} N_2, \quad N_2 = \sqrt{1 - p_2^2 \omega^{-2}}.$$

We substitute expression (8.16) into expressions (8.12) to obtain the components of the wave field:

$$E_x = \frac{i q_2}{n_0^2 U^2(t)} \psi_2; \quad H_y = -\frac{i \omega}{U(t)} \left(1 - \frac{i}{2\omega} \frac{\partial U}{\partial t} \right) \psi_2. \tag{8.17}$$

Expressions (8.11) and (8.17) describe two types of solutions of the nonstationary Maxwell equations. These solutions correspond to different dependences $U(t)$ defined implicitly by Eqns (8.7) and (8.15). We will now seek these dependences in an explicit form, assuming the function U to be equal to unity at the instant of commencement of the permittivity relaxation.

Problem (ii). We first consider the model of the nonstationary permittivity $U(t)$ described by Eqn (8.7). Upon the change $U = Q^2$ and the passage to the τ -variable (8.2), the solutions of Eqn (8.7) can assume one of two forms, depending on the sign of the constant p^2 :

$$U_1 = \left(\cos \frac{\tau}{T_1} + M_1 \sin \frac{\tau}{T_1} \right)^2, \quad p^2 = -T_1^2 < 0, \tag{8.18}$$

$$U_2 = \left(\cosh \frac{\tau}{T_2} + M_2 \sinh \frac{\tau}{T_2} \right)^2, \quad p^2 = T_2^2 > 0. \tag{8.19}$$

Here, M_1 and M_2 are free parameters of the models and T_1 and T_2 are the characteristic permittivity relaxation times.

We emphasize: it is the parameter τ rather than the real time t that appears in expressions (8.18) and (8.19). To obtain the dependences $U(t)$ in real time, one can resolve these formulas for τ and substitute the result into the definition of τ (8.2). The mathematical formalism of this approach is similar to the determination of U in the problems on nonuniform dielectrics (2.29)–(2.33). Specifically, using expression (8.18), we obtain

$$\frac{\tau}{T_1} = \arccos \sqrt{\frac{U_1}{1 + M_1^2}} + \arcsin \frac{M_1}{\sqrt{1 + M_1^2}}. \tag{8.20}$$

By differentiating expressions (8.20) and (8.2) and equating the expressions for the differentials $d\tau$, we obtain the equation that characterizes the dependence of U on the real time t :

$$\frac{\partial U_1}{\partial t} = \pm \frac{2}{T_1} \sqrt{\frac{1 + M_1^2}{U_1}} - 1. \tag{8.21}$$

The plus and minus signs correspond to the ascending and descending branches of the function U_1 , respectively.

The ascending branch of the solution of Eqn (8.21) describes the growth of the function from the value $U_1 = 1$ to the peak $U_{\max} = 1 + M_1^2$:

$$\frac{t}{T_{11}} = \frac{1}{2} \left[M_1 - \sqrt{U_1(1 + M_1^2 - U_1)} + (1 + M_1^2) \left(\arcsin \sqrt{\frac{U_1}{1 + M_1^2}} - \arcsin \frac{1}{\sqrt{1 + M_1^2}} \right) \right]. \tag{8.22}$$

The duration of this process \tilde{t}_1 is

$$\frac{\tilde{t}_1}{T_{11}} = \frac{1}{2} \left[M_1 + (1 + M_1^2) \arccos \frac{1}{\sqrt{1 + M_1^2}} \right]. \tag{8.23}$$

The solution of Eqn (8.21) that corresponds to the decrease of the function from the value U_{\max} to $U = 1$ is of the form

$$\frac{t - \tilde{t}_1}{T_{12}} = \frac{1}{2} \left[\sqrt{U_1(1 + M_1^2 - U_1)} + (1 + M_1^2) \left(\frac{\pi}{2} - \arcsin \sqrt{\frac{U_1}{1 + M_1^2}} \right) \right]. \tag{8.24}$$

Here, T_{11} and T_{12} are the characteristic increase and decrease times of the function $U_1(t)$. It is significant that these times may be different; for $T_{11} \neq T_{12}$, the shape of the $U_1(t)$ curve is asymmetric about the peak U_{\max} .

The model $U(t)$ in the case of expression (8.19) can be found in a similar way. The decrease of the function $U = U_2$ from the initial value $U = 1$ to the minimum $U_{\min} = 1 - M_2^2$ (it is assumed that $M_2^2 < 1$) and the duration \tilde{t}_2 of this decrease are determined by the expressions

$$\frac{t}{T_{21}} = \frac{1}{2} \left[M_2 - \sqrt{U_2(U_2 + M_2^2 - 1)} + (1 - M_2^2) \left(\operatorname{arcosh} \frac{1}{\sqrt{1 - M_2^2}} - \operatorname{arcosh} \sqrt{\frac{U_2}{1 - M_2^2}} \right) \right], \tag{8.25}$$

$$\frac{\tilde{t}_2}{T_{21}} = \frac{1}{2} \left[M_2 + (1 - M_2^2) \operatorname{arcosh} \frac{1}{\sqrt{1 - M_2^2}} \right]. \tag{8.26}$$

The ascending branch of the $U(t)$ curve is given by the function

$$\frac{t - \tilde{t}_2}{T_{22}} = \frac{1}{2} \left[\sqrt{U_2(U_2 + M_2^2 - 1)} + (1 - M_2^2) \operatorname{arcosh} \sqrt{\frac{U_2}{1 - M_2^2}} \right]. \tag{8.27}$$

Here, T_{21} and T_{22} are the characteristic relaxation times.

By alternating the branches U_1 and U_2 , provided that their tangency is smooth, it is possible to model continuous oscillations of the permittivity $\varepsilon(t)$. The solutions that describe these branches contain two free parameters — the quantity M , which determines the oscillation amplitude and shape, and the characteristic time T . The conditions for the

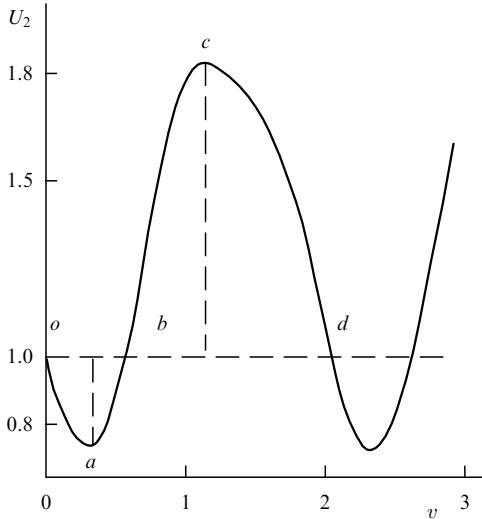


Figure 17. Nonharmonic oscillations of the function $U_2(v)$, $v = tT_{11}^{-1}$, represented by the solutions (8.23)–(8.27) for the parameter values $M_1 = 0.4$ and $M_2 = 0.6$. The branches oa , ab , bc , and cd determined by these solutions correspond to the characteristic times $T_{12} = 0.5T_{11}$, $T_{21} = 0.75T_{11}$, and $T_{22} = 1.5T_{11}$.

smoothness of tangency impose limitations on the values of M for the neighboring branches. Specifically, for a tangency at the level $U = 1$, these quantities are related as follows:

$$\frac{M_1}{M_2} = \frac{T_{12}}{T_{21}}. \tag{8.28}$$

An example of nonsinusoidal oscillations of the function $U(t)$ described by formulas (8.22)–(8.28) is given in Fig. 17.

Unlike the above $U(t)$ model defined by Eqn (8.7), the solution of Eqn (8.15) describes a simpler dependence $U(t)$ similar to the model (2.11):

$$U(t) = 1 + \frac{s_1 t}{t_1} + \frac{s_2 t^2}{t_2^2}. \tag{8.29}$$

Here, t_1 and t_2 are the characteristic relaxation times; the quantity p_2^2 (8.15), t_1 and \tilde{t}_2 are related as follows

$$p_2^2 = \frac{s_2}{\tilde{t}_2^2} - \frac{s_1^2}{4t_1^2}, \quad s_1 = 0, \pm 1, \quad s_2 = 0, \pm 1. \tag{8.30}$$

The function (8.29) can describe both monotonic permittivity variations and the formation of an extremum U_m at some point in time, depending on the values of the parameters s_1 , s_2 , t_1 , and t_2 .

The smooth tangency of the curves (8.29) and the curves obtained in the solution of Eqn (8.21) makes it possible to further extend the scope of exactly solvable models of the propagation of electromagnetic waves in nonstationary dielectrics.

Problem (iii). To investigate the reflection of a plane wave incident normally from vacuum onto the surface of a nonstationary medium, we represent the function ψ_0 , which describes the field in vacuum, as

$$\psi_0 = A_0 \exp[i(k_0 z - \omega t)]. \tag{8.31}$$

This function satisfies the field equations (8.6) and (8.14) for vacuum ($n_0 = 0$, $U = 1$). The reflectivity is found from the

conditions of continuity for the electric and magnetic field components at the medium boundary $z = 0$. In the description of the wave reflection by the medium's surface (8.7), the field components in vacuum can be found by substituting expression (8.31) into expressions (2.4). The field components in the medium are, in the model considered (see Fig. 17), defined by relations (8.11). By using the continuity conditions, it is possible to express the reflectivity for this medium as

$$R_1 = \frac{1 - n_1}{1 + n_1}; \quad n_1 = n_0 U_1(t) N_1 \left(1 - \frac{i}{2\omega} \frac{\partial U_1}{\partial t} \right). \tag{8.32}$$

For the model (8.29), the reflectivity is calculated in a similar way:

$$R_2 = \frac{1 - n_2}{1 + n_2}; \quad n_2 = n_0 U_2(t) N_2 \left(1 + \frac{i}{2\omega} \frac{\partial U}{\partial t} \right)^{-1}. \tag{8.33}$$

Formulas (8.32) and (8.33) are the generalization of the Fresnel formulas to the case of reflection by a nonstationary medium. These results reveal the dynamic nature of the reflection: the coefficients $R_{1,2}$ depend not only on the instantaneous values of $U(t)$, but also on their derivatives. In the special case where the time dependence disappears ($U_{1,2} = 1$, $N_{1,2} = 1$), expressions (8.32) and (8.33) pass into the well-known Fresnel formula for a stationary medium

$$R = (1 - n_0)(1 + n_0)^{-1}.$$

The imaginary parts of the complex reflectivities describe the spectral changes in the wave reflected from a nonstationary medium. For instance, in the reflection from the medium (8.29), the reflectivity R_2 (8.33) can be written as $R_2 = |R_2| \exp(i\varphi)$, where φ is the time-dependent phase:

$$\begin{aligned} \sin \varphi &= n_0 N_2 U_2 U_2' \omega A^{-1/2}, \quad U_2' = \frac{\partial U_2}{\partial t}, \\ A &= \left[N_2^2 - (n_0 U_2)^2 - \left(\frac{n_0 U_2 U_2'}{2\omega} \right)^2 \right]^2 + \left(\frac{n_0 N_2 U_2 U_2'}{\omega} \right)^2. \end{aligned} \tag{8.34}$$

We determine the frequency perturbation of the reflected wave $\Delta\omega$, which is caused by the time dependence of the phase φ (8.34), by the formula

$$\frac{\Delta\omega}{\omega} = -\frac{1}{\omega} \frac{\partial \varphi}{\partial t} \tag{8.35}$$

and differentiate the expression (8.34) for φ to obtain the frequency perturbation in the reflection from a medium with $\varepsilon(t) = n_0^2 U^2(t)$

$$\begin{aligned} \frac{\Delta\omega}{\omega} &= -\frac{n_0 N_2}{\omega^2 \sqrt{A}} \left[U_2 U_2'' + (U_2')^2 - \frac{A' U U''}{2A} \right] \\ &\times \left[1 - \left(\frac{n_0 N_2}{\omega} \frac{U U'}{\sqrt{A}} \right)^2 \right]^{-1/2}. \end{aligned} \tag{8.36}$$

The application of the results obtained can be exemplified by the problem of spectrum broadening in the wave reflection from a semiconductor in which the carrier density rises steeply owing to the ionization induced by a high-power laser beam.

We represent the time-dependent dielectric permittivity as [24]

$$\varepsilon(t) = \varepsilon_L \left[1 - \frac{\Omega_0^2 K(t)}{\omega^2} \right] = \varepsilon_L \left(1 - \frac{\Omega_0^2}{\omega^2} \right) U^2(t). \quad (8.37)$$

Here, ε_L is the lattice contribution to the permittivity and the dimensionless quantity $K(t)$ satisfies the condition $K|_{t=0} = 1$. The function $U(t)$ is assumed to be of the form (8.29); in this case, the ionization build-up corresponds to a decrease of $U(t)$. We consider the mode whereby the ionization peaks within a time T and thereafter retains a constant magnitude $N_m = N_0 K_m$; in this case, the function U reaches a minimum $U_m < 1$. To find the values of the parameters t_1 and t_2 in the model (8.29), we take into account that the following conditions are fulfilled at the moment of time $t = T$:

$$\begin{aligned} \frac{\partial U}{\partial t} \Big|_{t=T} &= 0, \\ U_m^2 \Big|_{t=T} &= \left(1 - \frac{t_2^2}{4t_1^2} \right)^2 = \left(1 - \frac{\Omega_0^2 K_m}{\omega^2} \right) \left(1 - \frac{\Omega_0^2}{\omega^2} \right)^{-1}. \end{aligned} \quad (8.38)$$

We obtain the values of t_1 , t_2 , and p_2^2 from Eqns (8.38):

$$t_1 = \frac{T}{2(1 - U_m)}; \quad t_2 = \frac{T}{\sqrt{1 - U_m}}; \quad p_2^2 = \frac{U_m(1 - U_m)}{T^2}. \quad (8.39)$$

The relative broadening of the spectrum of the reflected waves is shown in Fig. 18. The red frequency shift of the reflected wave is related to a decrease of the semiconductor index of refraction due to the rise in the carrier density.

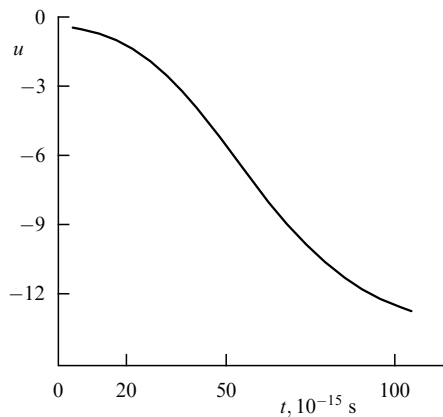


Figure 18. Nonstationary spectrum broadening of the $\lambda = 30 \mu\text{m}$ wave ($\Delta\omega\omega^{-1} = u \times 10^3$), which is reflected from the InSb plasma surface ($\varepsilon_L = 12.25$; $N_0 = 10^{17} \text{ cm}^{-3}$), in response to a hundred-fold increase in the carrier density within the characteristic time $T = 100 \times 10^{-15} \text{ s}$.

In conclusion of this analysis, we draw the reader's attention to the wide diversity of exactly solvable models of time-dependent permittivity composed of different branches of the functions U_1 and U_2 . The flexibility of such a modeling is ensured by the existence of no less than two free parameters for each branch of the functions U_1 and U_2 .

Employing the models considered above permits constructing broad classes of exact analytical solutions of the Maxwell equations for nonstationary dielectrics. These solutions describe the time evolution of the fields for an

arbitrary ratio between the wave period T and the medium relaxation time t_0 . We note some features of this evolution.

1. Dynamic effects (8.32), (8.33) related to the first and second derivatives of the time dependence $\varepsilon(t)$ may be significant in the wave reflection by a nonstationary medium. These effects resemble the effect of the profile gradient and curvature on the wave reflection from a nonuniform dielectric, which was already noted in Section 4.

2. Formulas (8.9) and (8.16) are evidence for the formation of normal and anomalous dispersion in nonstationary media. These dispersion effects, characterized by the factors N_1 and N_2 , are determined by the finite permittivity relaxation times.

If the characteristic times t_1 and t_2 in the $U(t)$ model (8.29) are related as $t_2^2 = (4t_1^2)^{-1}$, the parameter (8.30), which determines the medium dispersion, vanishes and the dispersion factor is equal to unity in this case. Therefore, in the special case where the dependence (8.29) is

$$U_2 = \left(1 + \frac{s_1 t}{2t_1} \right)^2, \quad (8.40)$$

the dispersion arising from the finiteness of the $\varepsilon(t)$ relaxation times disappears.

3. The dispersion equations (8.9) and (8.16) for waves in nonstationary media resemble the dispersion equation for high-frequency waves in a plasma; in this case, the quantities p^2 are similar to the plasma frequency squared. For $p^{-2}\omega^2 = 1$, a total wave reflection from a nonstationary dielectric occurs.

9. Telegraph equation for media with time-dependent conductivities

In Section 8, the influence of fast carrier density variations in a dielectric on the wave dispersion in the optical and near-IR ranges was considered without taking account of the medium conduction and the wave absorption. However, the conduction may play an important role if the contribution of the unperturbed carrier density N to $\text{Re}\varepsilon$ is not large and the perturbations of N under consideration do not change this relation. In this case, $\text{Re}\varepsilon \sim \varepsilon_L$, and the perturbations of the conductivity σ vary in direct proportion with $N(t)$. In this case, the effect of variable carrier density on both the dispersion and the wave absorption should be taken into account.

Let us consider the case where a wave is normally incident onto the surface of such a nonstationary conductor. We resort to Eqns (8.3) once again, now assuming that [38]

$$D_x = \varepsilon_L E_x + \int_0^t \sigma(t') E_x dt'. \quad (9.1)$$

By representing the variable conductivity $\sigma(t)$ in terms of the dimensionless function $P(t)$ as

$$\sigma(t) = \sigma_0 P(t), \quad P(t) \Big|_{t=0} = 1 \quad (9.2)$$

and expressing the field components E_x and H_y in terms of the function ψ (2.4), it is possible to reduce the system (8.3) to the equation

$$\frac{\partial^2 \psi}{\partial z^2} - \frac{1}{v^2} \frac{\partial^2 \psi}{\partial t^2} = \frac{P(t)}{v^2 T} \frac{\partial \psi}{\partial t}. \quad (9.3)$$

In Eqn (9.3), v and T are the wave velocity and the characteristic field settling time in the unperturbed medium:

$$v = \frac{c}{\sqrt{\epsilon_L}}; \quad T = \frac{\epsilon_L}{\sigma_0}. \tag{9.4}$$

Unlike the conventional telegraph equation, the coefficient in the right-hand side of Eqn (9.3) is an unknown function of time [39]. To determine the form of this function, allowing an exact analytical solution of Eqn (9.3), we will seek a solution of Eqn (9.3) in the form

$$\psi = F(z, t) \exp\left(-\int_0^t \alpha(t') dt'\right). \tag{9.5}$$

We substitute expression (9.5) into Eqn (9.3) to obtain an equation for the function F :

$$\frac{\partial^2 F}{\partial z^2} + \frac{\omega^2}{v^2} F = \frac{1}{v^2} \left[AF + B \frac{\partial F}{\partial t} \right], \tag{9.6}$$

$$A = \alpha^2 - \frac{\partial \alpha}{\partial t} - \frac{\alpha U}{T}, \quad B = \frac{P(t)}{T} - 2\alpha. \tag{9.7}$$

We impose additional conditions

$$A = 0, \quad B = \text{const} = \frac{1}{t_0}. \tag{9.8}$$

Then, Eqn (9.6) reduces to the conventional form of the telegraph equation with constant coefficients:

$$\frac{\partial^2 F}{\partial z^2} - \frac{1}{v^2} \frac{\partial^2 F}{\partial t^2} = \frac{1}{v^2 t_0} \frac{\partial F}{\partial t}. \tag{9.10}$$

The meaning of the parameter t_0 , which has the dimensionality of time, will be established below.

We now seek the time dependence of the conductivity $P(t)$ and the function $\alpha(t)$ from Eqns (9.7) and (9.8). Representing the function α in the form (9.7)

$$\alpha = \frac{1}{2} \left(\frac{P}{T} - \frac{1}{t_0} \right) \tag{9.11}$$

and substituting expression (9.11) into the condition (9.8), we obtain an equation for the function $U(t)$. The function $U(t)$ is represented in either of two forms

$$P_1 = \left[\gamma \tanh\left(\text{artanh } \gamma^{-1} + \frac{t}{2t_0}\right) \right]^{-1}, \quad \gamma = \frac{t_0}{T} > 1, \tag{9.12}$$

$$P_2 = \gamma^{-1} \tanh\left(\text{artanh } \gamma + \frac{t}{2t_0}\right), \quad \gamma = \frac{t_0}{T} < 1 \tag{9.13}$$

depending on the ratio between the times t_0 and T (9.4). One can see from expressions (9.12) and (9.13) that the parameter t_0 characterizes the conductivity relaxation time. Figure 19 represents the models (9.12) and (9.13); these describe the ‘saturation’ of conductivity, which increases or decreases with time. Curve I , in particular, illustrates the conductivity build-up mode related to the rise of carrier density $\sigma \sim N(t)$. In a time $t \gg 2t_0$, the conductivity reaches the value $P = \gamma^{-1}$.

We now construct the function ψ (9.5), which describes the field in a nonstationary medium. The solution of the

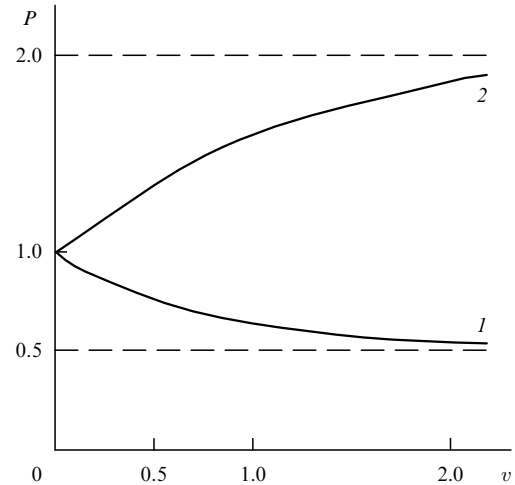


Figure 19. Normalized conductivity P as a function of time $v = tt_0^{-1}$. Curves 1 and 2 correspond to the values $\gamma = 0.5$ (9.12) and $\gamma = 2$ (9.13). The dashed lines correspond to the asymptotic values $P = \gamma^{-1}$ for $v \gg 1$.

telegraph equation (9.10) for the function F is of the form

$$F = \exp[i(qz - \omega t)], \tag{9.14}$$

$$q = \frac{\omega}{c} n_\sigma, \quad n_\sigma = \sqrt{\epsilon_L} \sqrt{1 + i(\omega t_0)^{-1}}.$$

Substituting the values of $P(t)$ from expressions (9.12) and (9.13) and then calculating the exponential factor in expression (9.5), we obtain, for instance, for a fast relaxation ($\gamma < 1$)

$$\exp\left[-\int_0^t \alpha(t') dt'\right] = \frac{1}{\sqrt{1 - \gamma^2}} \frac{\exp(t/2t_0)}{\cosh(\text{artanh } \gamma + t/2t_0)}. \tag{9.15}$$

By combining the results (9.14) and (9.15), after algebraic rearrangements we arrive at a simple solution of the nonstationary telegraph equation (9.3) corresponding to the model $P_1(t)$ (9.12):

$$\psi = 2\Delta^{-1} \exp[i(qz - \omega t)], \tag{9.16}$$

$$\Delta = 1 + \gamma + (1 - \gamma) \exp\left(-\frac{t}{t_0}\right).$$

The substitution of the solution (9.16) into relationships (2.4) gives the electric and magnetic components of the wave field in the conductor (9.12):

$$E_x = \frac{i\omega}{c} \left[1 - \frac{i(1 - \gamma)}{\Delta \omega t_0} \exp\left(-\frac{t}{t_0}\right) \right] \psi, \tag{9.17}$$

$$H_y = \frac{i\omega}{c} n_\sigma \sqrt{\epsilon_L} \sqrt{1 + i(\omega t_0)^{-1}} \psi. \tag{9.18}$$

Using the boundary conditions at the conductor boundary, we obtain the complex reflectivity R :

$$R = \left[1 + \frac{i(1 - \gamma)}{\omega t_0 \Delta} \exp\left(-\frac{t}{t_0}\right) - q \right] \times \left[1 + \frac{i(1 - \gamma)}{\omega t_0 \Delta} \exp\left(-\frac{t}{t_0}\right) + q \right]^{-1}, \quad \lim_{t \gg t_0} R = \frac{1 - q}{1 + q}. \tag{9.19}$$

The amplitude and phase of the reflected wave change with time, these changes developing in a characteristic time t_0 . For times $t \gg t_0$, the amplitude and phase of the coefficient R tend to constant values determined by formula (9.19).

It is interesting to note the special case of the model under discussion which corresponds to the value $B = 0$ in the system of equations (9.8). In this case, Eqn (9.10) for the function F assumes the form of a wave equation in free space:

$$\frac{\partial^2 F}{\partial z^2} - \frac{1}{v^2} \frac{\partial^2 F}{\partial t^2} = 0. \quad (9.20)$$

The solution of this equation is an arbitrary doubly differentiable function $F(t - zv^{-1})$. The function $P(t)$, which can be determined from the conditions $A = 0$ and $B = 0$, decreases according to the formula

$$P = \left(1 + \frac{t}{2T}\right)^{-1}. \quad (9.21)$$

Upon calculating the exponential factor in the function ψ (9.5) for the model (9.21), we obtain the solution of the telegraph equation in the form

$$\psi = \left(1 + \frac{t}{2T}\right)^{-1} F\left(t - \frac{z}{v}\right). \quad (9.22)$$

The solution (9.22) resembles a wave which traverses a communication line free of dispersion distortions [23]. The substitution of expression (9.22) into Eqns (2.4) shows that the envelope of the magnetic component of the wave field retains its shape as it propagates through a nonstationary conductor (9.21).

The time-dependent conductivity $\sigma(t) = \sigma_0 P(t)$ (9.12), (9.13) and the electromagnetic field (9.17), (9.18) are an example of an exactly solvable model of a nonstationary conductor. The dispersion field distortions in this medium are determined by the ratio between the characteristic relaxation times T and t_0 . A search for solutions of the nonstationary telegraph equation (9.3) is of interest for the analysis of transmission lines with a time-dependent impedance.

10. Conclusions. Phase coordinates in problems of the radiophysics of guidance systems, nonlinear optics, and quantum mechanics

The exact solutions of the Maxwell equations for nonuniform and nonstationary media were constructed above with the aid of new variables — the phase coordinates η (2.6) and τ (8.2). These variables allowed the complex structure of the electromagnetic fields in the media under consideration to be represented as harmonic waves in the spaces (η, t) and (z, τ) . This approach is also possible in the solution of wave problems in other branches of physics. Several examples of such applications are discussed below.

I. Long line with nonuniformly distributed parameters. As is well known, the distribution of the current I and the voltage V in a loss-free distributed-parameter line is described by the pair of equations [23]

$$\frac{\partial V}{\partial z} + L \frac{\partial I}{\partial t} = 0, \quad (10.1)$$

$$\frac{\partial I}{\partial z} + C \frac{\partial V}{\partial t} = 0. \quad (10.2)$$

Here, L and C are the line inductance and capacitance per unit length; the resistance and the leakage current are neglected for simplicity.

Within the framework of the system (10.1), (10.2) we consider the case where L and C are nonuniformly distributed. For instance, let the inductance vary lengthwise along the line according to the law

$$L = L_0 U^2(z), \quad U\Big|_{z=0} = 1. \quad (10.3)$$

The solution of the system (10.1), (10.2) can be sought in two ways.

1. By introducing an auxiliary function ψ through the relationships

$$I = -C \frac{\partial \psi}{\partial t}, \quad V = \frac{\partial \psi}{\partial z}, \quad (10.4)$$

we obtain the following wave equation for ψ :

$$\frac{\partial^2 \psi}{\partial z^2} - \frac{U^2(z)}{V^2} \frac{\partial^2 \psi}{\partial t^2} = 0. \quad (10.5)$$

Eqn (10.5) coincides in form with Eqn (2.5), and both are subsequently analyzed in the same way: we introduce the phase coordinate η (2.6), find the function ψ (2.10) for the inductance distribution (2.11), and lastly calculate the current and voltage envelopes (10.4).

2. By expressing, unlike relationships (10.4), the current and voltage in terms of an auxiliary function Θ through the relationships

$$I = \frac{1}{L_0 U^2} \frac{\partial \Theta}{\partial z}, \quad V = -\frac{\partial \Theta}{\partial t}, \quad (10.6)$$

we reduce the system (10.1), (10.2) to an equation which coincides, upon the change $V^2 \rightarrow c^2 n_0^{-2}$, with Eqn (2.20). We next construct the function Θ as a traveling wave in the variables (η, t) (2.26), employ the distribution $U(z)$ shown in Fig. 2, etc. The derivation of the reflectivities and the matching of line segments are performed by analogy with the calculations in Section 4.

A wave equation with a time-dependent velocity of the type (10.5) arises in the description of a number of processes in a nonuniform continuous medium. In particular, this equation describes the Alfvén waves propagating along the magnetic field in a variable-density plasma [40]. The cutoff frequency for the Alfvén waves was found in Ref. [41] for several plasma density profiles.

II. Nonlinear Schrödinger equation for a medium with a parabolic profile of the refractive index. As is well known, the self-action of waves in Kerr media is described by the nonlinear Schrödinger equation (NSE). If such a self-action develops in a medium with a nonuniform refractive index, the solution of the NSE is hampered owing to the coordinate dependence of the coefficients. However, in this case the coordinate dependence can also be eliminated by a special transformation of the variables and the function in this equation.

We consider this approach for a Kerr medium wherein the refractive index obeys the parabolic distribution

$$n(\rho) = n_0 - \frac{g^2 \rho^2}{2}. \quad (10.7)$$

The nonlinear Schrödinger equation that describes the evolution of the envelope E of a pulse traveling in the z -direction in the medium (10.11) is of the form

$$i \frac{\partial E}{\partial z} = -\frac{1}{2\kappa} \left(\frac{\partial^2 E}{\partial x^2} + \frac{\partial^2 E}{\partial y^2} \right) + \frac{\kappa g^2 \rho^2}{2} E - \frac{n_2 \kappa |E|^2 E}{n_0} = 0. \tag{10.8}$$

Here, n_2 is the Kerr coefficient and $\kappa = \omega n_0 c^{-1}$. We go over to the normalized variables

$$E = E_0 \psi, \quad x_1 = \sqrt{s} x a_0^{-1}, \quad y_1 = \sqrt{s} y a_0^{-1}, \\ z_1 = s z (\kappa a_0^2)^{-1}, \quad v^2 = \kappa a_0^2 g s^{-1}, \quad s = n_2 E_0^2 \kappa^2 a_0^2 n_0^{-1} \tag{10.9}$$

(a_0 is the effective radius of the wave beam and E_0 is the field amplitude) and substitute expressions (10.9) in Eqn (10.8) to rewrite the NSE in the dimensionless form

$$i \frac{\partial \psi}{\partial z_1} = -\frac{1}{2} \left(\frac{\partial^2 \psi}{\partial x_1^2} + \frac{\partial^2 \psi}{\partial y_1^2} \right) + \frac{v^2}{2} (x_1^2 + y_1^2) \psi - |\psi|^2 \psi. \tag{10.10}$$

Eqn (10.10) describes, in particular, the nonlinear field dynamics in a light guide with a parabolic profile of $n(\rho)$.

Extending the approach employed in Section 2, we introduce a new function f to be found (2.21) and the η -variable (2.6) using an auxiliary function U :

$$\psi = f \sqrt{U}; \quad U = \cos^{-2}(v z_1); \\ \eta = \frac{1}{v} \tan(v z_1). \tag{10.11}$$

This transformation brings Eqn (10.10) to the form

$$i \left[\frac{\partial f}{\partial \eta} \frac{1}{\cos^2(v z_1)} - v f \tan(v z_1) \right] \\ = -\frac{1}{2} \left(\frac{\partial^2 f}{\partial x_1^2} + \frac{\partial^2 f}{\partial y_1^2} \right) + \frac{v^2}{2} (x_1^2 + y_1^2) f - \frac{|f|^2 f}{\cos^2(v z_1)}. \tag{10.12}$$

We introduce a new function φ [42] to eliminate from Eqn (10.10) the term which contains the sum of squares:

$$f = \varphi \left[\frac{x_1}{\cos(v z_1)}, \frac{y_1}{\cos(v z_1)}, \eta \right] \exp \left[-\frac{v^2}{2} (x_1^2 + y_1^2) \right]. \tag{10.13}$$

We substitute expression (10.13) into Eqn (10.12) to obtain the nonlinear Schrödinger equation in the form

$$i \frac{\partial \varphi}{\partial \eta} = -\frac{1}{2} \left(\frac{\partial^2 \varphi}{\partial x_1^2} + \frac{\partial^2 \varphi}{\partial y_1^2} \right) - |\varphi|^2 \varphi. \tag{10.14}$$

Therefore, the transformations (10.11)–(10.13) convert the nonuniform NSE (10.10) into an equation with constant coefficients (10.14), which significantly alleviates the study of the nonlinear modes of wave beam propagation.

III. Energy levels of a particle in a potential well. The discrete energy levels ε_n of a particle in the simple model of a square potential well of width a are determined by the well-known formula

$$\varepsilon_n = \frac{\pi^2 n^2 \hbar^2}{2ma^2}. \tag{10.15}$$

In this model, however, the derivatives of the potential $U(z)$ exhibit jumps at the bottom of the well ($U = 0$), at the points

$z = 0$ and $z = a$. To find the energy levels for a potential profile of finite width, as in the case of formula (10.15), which, however, has no corners, we can use the function $U_1 = U^2(z)$, where the dependence $U(z)$ is defined by expression (6.22) with $M = 0$.

The Schrödinger equation with a potential of this kind is of the form

$$\frac{\partial^2 \psi}{\partial z^2} + \frac{2m}{\hbar^2} \left[\varepsilon - \frac{U_0}{\cos^2(z/L)} \right] \psi = 0. \tag{10.16}$$

The potential is defined in the interval $z_1 \leq z \leq z_2$, where

$$z_1 = -\frac{\pi}{2} L; \quad z_2 = \frac{\pi}{2} L. \tag{10.17}$$

The U_1 function is shown in Fig. 20. This function has a minimum at the point $z_m = 0$:

$$U_1 \Big|_{z=z_m} = 1. \tag{10.18}$$

For high values of the potential U_1 , at which the well walls are nearly vertical, the profile $U_1(z)$ approximates a square potential well, being close to the parabola $U_1 = 1 + z^2 L^{-2}$ near the minimum $z = 0$.

To solve the Schrödinger equation (10.16), we introduce a new function f and a new dimensionless variable x :

$$f = \frac{\psi}{\sqrt{\cos(z/L)}}; \quad x = \frac{1}{L} \int_0^z \frac{dz'}{\cos(z'/L)}. \tag{10.19}$$

We substitute expressions (10.19) into Eqn (10.16) to obtain

$$\frac{\partial^2 f}{\partial x^2} + f \left[-q^2 + \frac{T}{\cosh^2 x} \right] = 0, \tag{10.20}$$

$$q^2 = \frac{1}{4} + \frac{2mU_0L^2}{\hbar^2}; \quad T = \frac{2mL^2\varepsilon}{\hbar^2} - \frac{1}{4}. \tag{10.21}$$

Eqn (10.20) bears a formal resemblance to the Schrödinger equation for the potential $\cosh^{-2}x$ [26]. However, unlike the traditional problem of level determination, the unknown energy levels ε appear, in the case of this potential, in the coefficient q^2 rather than in the constant T . By introducing

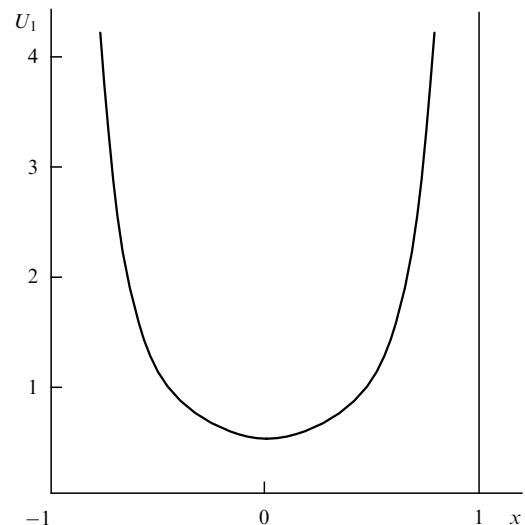


Figure 20. Potential well (2.16); $x = 2z(\pi L)^{-1}$, $U_0 = 0.5$.

once again a new function W and a new variable u ,

$$f = (\cosh x)^{-q} W, \quad u = \frac{1}{2}(1 - \tanh x), \quad (10.22)$$

we obtain a hypergeometric equation for the W function:

$$u(1-u) \frac{\partial^2 W}{\partial u^2} + [\gamma - u(1+\alpha+\beta)] \frac{\partial W}{\partial u} - \alpha\beta W = 0, \quad (10.23)$$

$$\gamma = 1 + q, \quad \alpha, \beta = \frac{1}{2} \left(1 + 2q \pm \sqrt{1 + 4T} \right). \quad (10.24)$$

To determine the range of values of the u -variable (10.22), we should calculate the values of the x -variable (10.19) which correspond to the points z_1 and z_2 (10.17) bounding the domain of definition of the potential $\cos^{-2}(zL^{-1})$ (10.16). The equalities

$$\sin \frac{z_2}{L} = 1, \quad \tan \frac{z_2}{2L} = 1 \quad (10.25)$$

are fulfilled at the point z_2 . By substituting the value z_2 into formula (6.35), we obtain $x_2 \rightarrow \infty$ and $u_2 = 0$. Similar calculations for the point z_1 give $x_1 \rightarrow -\infty$, $u_1 = 1$.

The solution of Eqn (10.2), finite for $u = 0$, is the hypergeometric function $W(\alpha, \beta, \gamma, u)$. For this solution to remain finite at $u = 1$, the following conditions should be fulfilled:

$$s(s+1) = T, \quad q - s = -n, \quad n = 0, 1, 2, \dots \quad (10.26)$$

By uncovering the values of the parameters q and T (10.21), we obtain the following formula which determines the energy level spectrum ε_n of a particle in the potential well depicted in Fig. 20:

$$\varepsilon_n = \frac{\hbar^2}{8mL^2} \left(1 + 2n + \sqrt{1 + \frac{8mL^2 U_0}{\hbar^2}} \right)^2. \quad (10.27)$$

We note several features of this spectrum:

(1) the value of the parameter U_0 , which characterizes the minimum of the potential U_1 , is arbitrary in the range $U_0 > 0$;

(2) unlike the square potential well (10.15), where the lowest energy level corresponds to the value $n = 1$, the lowest level in the spectrum (10.27) corresponds to $n = 0$;

(3) by introducing the quantity a , which determines the well width (10.17), into formula (10.27) and neglecting the rooted terms, it is possible to obtain the spectrum for high n values:

$$\varepsilon_n = \frac{n^2 \hbar^2}{2mL^2} = \frac{\pi^2 n^2 \hbar^2}{2ma^2}. \quad (10.28)$$

As one could expect, in the limit of high quantum numbers expression (10.27) coincides with the spectrum of an infinitely deep square potential well (10.15).

In the opposite limiting case [$U_0 \gg \hbar^2(8mL^2)^{-1}$], the spectrum (10.27) gives for low-lying energy levels

$$\varepsilon_n = U_0 + \hbar\omega_0 \left(n + \frac{1}{2} \right), \quad \omega_0 = \sqrt{\frac{2U_0}{mL^2}}. \quad (10.29)$$

As is well known, formula (10.29) describes the spectrum of a harmonic oscillator. Therefore, two model problems frequently used in quantum mechanics — the energy spectrum of a particle in a square potential well (10.28) and the energy

spectrum of a harmonic oscillator (10.29) — are special cases of the spectrum (10.27).

In summary, it should be noted that the problems of electromagnetic wave dispersion caused by the nonuniformity or the nonstationary state of the medium have been considered here for simple one-dimensional problems. The unified approach to such problems based on the use of new variables — phase coordinates — allowed the construction of exact analytical solutions of the Maxwell equations for broad classes of coordinate- or time-dependent continuous permittivity distributions. The flexibility of these models stems from the existence of several free parameters characterizing the nonuniformity scale lengths or the material relaxation times. In the new variables, the spatiotemporal structure of electromagnetic fields is described in some cases by sinusoidal waves and elementary functions while the dispersion is determined by waveguide-type formulas.

In the consideration of more complex two- and three-dimensional problems of wave reflection and diffraction, the approach proposed here is beneficial to the physical interpretation of the results obtained through computer simulations. Also of interest are the results of combined (analytical and numerical) research into such problems and their applications, for instance:

— the influence of a permittivity gradient on the reflection of waves incident obliquely on a plane dielectric surface [43]; this effect is employed to monitor the $\varepsilon(z)$ distribution in thin films;

— the effect of a double curvature of the reflecting surface, which is responsible for the effective nonuniformity of the near-surface layers, on wave reflection [44]. This effect determines corrections to the Fresnel formulas related to the finite wavelength;

— the localization of the near-surface light waves near the equator of a glass microsphere due to the variation of the phase path deep in the sphere [45]; this effect is of interest in the formation of high- Q microcavities.

In view of the flexibility of the exactly solvable models of $\varepsilon(z)$ and $\varepsilon(t)$ considered here and the ease of the corresponding solutions, the following steps can be contemplated to advance this approach:

1. The generalization of the analytical methods developed for isotropic nonuniform media to the problems of anisotropic and gyrotropic media, to the problems of magneto-optics in particular. Particularly, in the analysis of the Faraday effect in the simple case of inward wave propagation along the magnetic field (the z -axis) in a variable-density plasma ($z \geq 0$) described by model (6.1), the fields of ordinary and extraordinary waves can be expressed in terms of the function ψ_{\pm} :

$$E_{\pm} = E_x \pm iE_y = \frac{i}{c} \frac{\partial \psi_{\pm}}{\partial t}, \quad H_{\pm} = H_x \pm iH_y = \frac{\partial \psi_{\pm}}{\partial z}. \quad (10.30)$$

Following the treatment of the similar problem for an isotropic medium (see Section 6), we introduce the phase path η and the functions $f_{\pm} = \psi_{\pm} U^{-1/2}$; in this case, the Maxwell equations for the ordinary f_+ and extraordinary f_- waves can be written as

$$\frac{\partial^2 f_{\pm}}{\partial \eta^2} + f_{\pm} \left[\frac{p_{\pm}^2}{U^2} - \frac{\omega \Omega_0^2}{\omega \pm \omega_H} \frac{\varepsilon_L}{bc^2} - \frac{1}{2U} \frac{\partial^2 U}{\partial \eta^2} + \frac{1}{4U^2} \left(\frac{\partial U}{\partial \eta} \right)^2 \right] = 0, \quad (10.31)$$

$$p_{\pm}^2 = \frac{\omega^2 \varepsilon_L}{c^2} \left[1 - \frac{\Omega_0^2}{\omega(\omega \pm \omega_H)} (1 - b^{-1}) \right].$$

Here, ω_H is the electron gyrofrequency and ε_L the part of the material permittivity independent of the electron density.

Consider, for instance, the wave propagation in the direction of density increase ($b < 0$, $b = -|b|$). We use the simple model $U(z) = 1 + za^{-1}$ (6.10) to obtain equations of the type (6.11) for the functions f_{\pm} , where the parameters q_{\pm}^2 (6.12) are

$$q_{\pm}^2 = \frac{1}{4} - \frac{\varepsilon_L a^2 \Omega_0^2 \omega}{c^2 |b| (\omega \pm \omega_H)}. \quad (10.32)$$

The structure of the wave field in the medium depends on the parameters p_{\pm}^2 and q_{\pm}^2 , which in turn depend on the spatial nonuniformity scale length a and the plasma density deep in the medium $W = 1 + |b|^{-1}$ (6.1). In particular, for $p_{\pm}^2 > 0$ and $q_{\pm}^2 > 0$, the medium is transparent for both the ordinary and extraordinary waves, and these wave fields can be expressed with the aid of expressions (10.30) in terms of the Hankel functions $H_{q_{\pm}}^{(1)}$ (6.13):

$$\psi_{\pm} = \sqrt{1 + \frac{z}{a}} H_{q_{\pm}}^{(1)} [p_{\pm}(a + z)] \exp(-i\omega t). \quad (10.33)$$

The interference of the waves E_+ and E_- in the medium is, as is well known, responsible for the rotation of the polarization plane (the Faraday effect). However, unlike the even rotation of this plane in a uniform plasma, the Faraday effect in the problem under consideration is characterized by an uneven rotation of the vectors \mathbf{E} and \mathbf{H} .

2. The selection of the transformations of coordinates which correspond to the given model of the medium's nonuniformity. Problems of the optics of nonuniform media were considered here with recourse to the transformations of the Maxwell equations involving the introduction of the η -variable and the function F (2.6). In this case, the η -variable has the meaning of the phase path in the medium. However, for some distributions of the nonuniform permittivity, it is advantageous to resort to more complex representations for the η -variable and the related function F . Thus, when considering the wave equation with a coordinate-dependent refractive index $n = n_0 U(z)$,

$$\frac{\partial^2 \psi}{\partial z^2} - \frac{U^2(z)}{V_0^2} \frac{\partial^2 \psi}{\partial t^2} = 0, \quad V_0 = \frac{c}{n_0}, \quad (10.34)$$

one can introduce a new function F and a new η -variable:

$$\psi = F U^p, \quad \eta = \int_0^z [U(z_1)]^q dz_1. \quad (10.35)$$

By representing the function U as $U = S^m$ and choosing the values $p = -m^{-1}$ and $q = 2m^{-1}$, it is possible to rewrite the wave equation (10.34) as

$$\frac{\partial^2 F}{\partial \eta^2} + F \left[-\frac{1}{S} \frac{\partial^2 S}{\partial \eta^2} + \frac{\omega^2}{V_0^2 S^{4-2m}} \right]. \quad (10.36)$$

We denote the characteristic nonuniformity scale length by L , introduce a new variable u , and prescribe the function S as

$$S = u^v, \quad u = \exp \frac{\eta}{L}, \quad v = \frac{1}{2-m}, \quad (10.37)$$

to rewrite Eqn (10.36) in the form of the Bessel equation:

$$\frac{\partial^2 F}{\partial u^2} + \frac{1}{u} \frac{\partial F}{\partial u} + F \left[\left(\frac{\omega L}{V_0} \right)^2 - \frac{1}{(2-m)^2 u^2} \right] = 0. \quad (10.38)$$

Here, the parameter m assumes any values with the exception of $m = 2$. The case $m = 2$ corresponds to the transformation (2.6) considered earlier.

The solutions of Eqn (10.38) are Bessel functions. The relationship between the u -variable and the z -coordinate can be found from expressions (10.35) and (10.37):

$$u = \left[1 - \frac{2}{m-2} \frac{z}{L} \right]^{1-2/m}. \quad (10.39)$$

The permittivity profile $\varepsilon(z) = n_0^2 U^2(z)$ is determined by substituting expression (10.39) into expression (10.37):

$$\varepsilon(z) = n_0^2 \left(1 - \frac{2}{m-2} \frac{z}{L} \right)^{-m}. \quad (10.40)$$

The solution of the wave equation (10.34) for the nonuniform dielectric (10.40) is of the form

$$\psi = \left(1 - \frac{2}{m-2} \frac{z}{L} \right)^{-m/2} \times \left[I_\nu \left(\frac{\omega L}{V_0} u \right) + K I_{-\nu} \left(\frac{\omega L}{V_0} u \right) \right] \exp(-i\omega t). \quad (10.41)$$

Here, K is a constant.

The family of solutions (10.41) is continuously dependent on the parameter m (with the exception of the value $m = 2$). In the special case where $m = 1$, the $\varepsilon(z)$ distribution (10.40) passes into the profile (1.2); the linear $\varepsilon(z)$ profile and the corresponding field structure determined by the Airy functions is described by expressions (10.40) and (10.41) for $m = -1$. Therefore, the transformation (10.35) defines the family of exact analytical solutions of the Maxwell equations for the $\varepsilon(z)$ profiles (10.40) containing the free parameters m and L . The subsequent extension of the classes of such coupled transformations is a burning problem of the optics of stratified and nonstationary media.

3. The construction of exactly solvable models of nonuniform and nonstationary media, simultaneously taking into account the dependences $\varepsilon(z)$ and $\sigma(z)$ or $\varepsilon(t)$ and $\sigma(t)$. The simultaneous inclusion of the dispersion effects caused by the nonuniformity and the nonstationary state of the medium, for instance, the effects of a nonuniformity in the form of a traveling wave of variations $\varepsilon(z, t)$.

Acknowledgements

The author gratefully acknowledges the discussion of these issues with Ya A Smorodinskiĭ (30 December 1917–16 October 1992) and expresses his gratitude to M Ablowitz, D Bolomei, F Bunkin, M Zuev, M Lisak, A Migus, E Meister, L Stenflo, G Petite, A Rukhadze, and S Kharosh for their invariable support of this work and interest in its results.

References

1. Rayleigh J W S P. *Lond. Math. Soc.* **11** 51 (1880)
2. Forsterling K. *Ann. Phys. - Leipzig* **11** 1 (1931)
3. Epstein L J J. *Opt. Soc. Am.* **42** 806 (1952)

4. Brekhovskikh L M, Godin O A *Akustika Sloistykh Sred* (Acoustics of Layered Media) (Moscow: Nauka, 1989); see also *Acoustics of Layered Media* I, II (Berlin: Springer-Verlag, 1990–1992)
5. Hartree D R P. *Roy. Soc. Lond. A Mat.* **131** 428 (1931)
6. Rydbeck O *Philos. Mag.* **34** 342 (1943)
7. Wait J R *Electromagnetic Waves in Stratified Media* (Oxford: Pergamon Press, 1970)
8. Agranovich V M, Ginzburg V L *Kristaloptika s Uchetom Prostranstvennoĭ Dispersii i Teoriya Eksitonov* (Crystal Optics with Spatial Dispersion, and Excitons) (Moscow: Nauka, 1965) [Translated into English (New York: Springer-Verlag, 1984)]
9. Kravtsov Yu A, Orlov Yu I *Geometricheskaya Optika Neodnorodnykh Sred* (Geometrical Optics of Inhomogeneous Media) (Moscow: Nauka, 1980) [Translated into English (Berlin: Springer-Verlag, 1990)]
10. Mikhailovskii A B *Teoriya Plazmennykh Neustoĭchivostei* (Theory of Plasma Instabilities) Vol. 2 *Neustoĭchivosti Neodnorodnoĭ Plazmy* (Instabilities of Nonuniform Plasmas) 2nd ed. (Moscow: Atomizdat, 1977) [Translated into English: *Theory of Plasma Instabilities* Vol. 2 (New York: Consultants Bureau, 1974)]
11. Averkov S I, Khronopulo Yu G *Izv. Vyssh. Uchebn. Zaved. Radiofiz.* (3) 818 (1960)
12. Felsen L B, Whitham G B *IEEE T. Antennas Propag.* **AP-18** 272 (1970)
13. Kuo S P, Zhang Y S *Phys. Fluids B – Plasma* **3** 2906 (1991)
14. Koretzky E, Kuo S P, Kim J J. *Plasma Phys.* **59** 315 (1998)
15. Shvartsburg A B *Impulse Time-Domain Electromagnetics of Continuous Media* (Boston: Birkhäuser, 1999)
16. Aleshkevich V A, Peterson V K *Pis'ma Zh. Eksp. Teor. Fiz.* **66** 323 (1997) [*JETP Lett.* **66** 344 (1997)]
17. Rottbrand K Z. *Angew. Math. Mech.* **78** 321 (1998)
18. Shvartsburg A, Petite G, Auby N *J. Opt. Soc. Am. B* **16** 966 (1999)
19. Shvartsburg A, Strand P, Weiland J *Phys. Scripta* **T-82** 81 (1999)
20. Bartuch U et al. *Opt. Commun.* **134** 49 (1997)
21. Sankur H, Southwell W *Appl. Optics* **23** 2770 (1984)
22. Kildemo M, Hinderi O, Dreviron B J. *Opt. Soc. Am. A* **14** 931 (1997)
23. Jackson J D *Classical Electrodynamics* 2nd ed. (New York: Wiley, 1975)
24. Shvartsburg A, Petite G, Hecquet P *J. Opt. Soc. Am. B* **17** 2267 (2000)
25. Abeles F *Ann. Phys. – New York* **5** 596 (1950)
26. Landau L D, Lifshitz E M *Kvantovaya Mekhanika. Nerelyativistskaya Teoriya* (Quantum Mechanics: Non-Relativistic Theory) (Moscow: Nauka, 1989) [Translated into English (Oxford: Pergamon Press, 1977)]
27. Whittaker E T, Watson G N *A Course of Modern Analysis* (Cambridge: University Press, 1927) [Translated into Russian (Moscow: Fizmatgiz, 1963)]
28. Hellberg R, Karlsson A, Tharning P *Smart Mater. Struct.* **1** 341 (1992)
29. Raether H *Surface Plasmons on Smooth and Rough Surfaces and on Gratings* (Berlin: Springer-Verlag, 1988)
30. Brodin G, Lundberg J J. *Plasma Phys.* **46** 299 (1991)
31. Monchicourt P et al. *J. Phys. – Condens. Mat.* **9** 5765 (1997)
32. Chian A et al. *Phys. Scripta* **T-60** 5 (1995)
33. Rosker M, Wise F, Tang C *Phys. Rev. Lett.* **57** 324 (1986)
34. Quere F et al. *Appl. Phys. B* **68** 459 (1999)
35. Askar'yan G A, Pogosyan V A *Zh. Eksp. Teor. Fiz.* **65** 1(7) 117 (1973) [*Sov. Phys. JETP* **38** 59 (1974)]
36. Tang N, Sutherland R L *J. Opt. Soc. Am. B* **14** 3412 (1997)
37. Shvartsburg A B *Kvantovaya Elektron.* (Moscow) **25** 201 (1998) [*Quantum Electron.* **28** 193 (1998)]
38. Ginzburg V L, Rukhadze A A *Elektromagnitnye Volny v Plazme* (Electromagnetic Waves in a Plasma) (Moscow: Nauka, 1974)
39. Masoliver J, Weiss G H *Phys. Rev E* **49** 3852 (1994)
40. Stenflo L, Shvartsburg A B, Weiland J *Contrib. Plasm. Phys.* **37** 393 (1997)
41. Musielak Z E, Fontenla J M, Moore R L *Phys. Fluids B – Plasma* **4** 13 (1992)
42. Manassah J T *Opt. Lett.* **17** 1259 (1992)
43. Lekner J *Physica A* **116** 235 (1982)
44. Snyder A, Mitchell D *Electron. Lett.* **9** 609 (1973)
45. Whitten W B, Barnes M D, Ramsey J M *J. Opt. Soc. Am. B* **14** 3424 (1997)